| | |
|---|---|
| **Titre:** Title: | Characterizing the Sacrificial Coating on Tools During Turning of TiMMCs |
| **Auteur:** Author: | Thi Luong Duong |
| **Date:** | 2021 |
| **Type:** | Mémoire ou thèse / Dissertation or Thesis |
| **Référence:** Citation: | Duong, T. L. (2021). Characterizing the Sacrificial Coating on Tools During Turning of TiMMCs [Master's thesis, Polytechnique Montréal]. PolyPublie. https://publications.polymtl.ca/6295/ |

**POLYTECHNIQUE MONTRÉAL**

affiliée à l'Université de Montréal

# Characterizing the Sacrificial Coating on Tools during Turning of TiMMCs

**THI LUONG DUONG**

Département de génie mécanique

Mémoire présenté en vue de l'obtention du diplôme de *Maîtrise ès sciences appliquées*

Génie mécanique

Avril 2021

**POLYTECHNIQUE MONTRÉAL**

affiliée à l'Université de Montréal

Ce mémoire intitulé :

**Characterizing the Sacrificial Coating on Tools during Turning of TiMMCs**

présenté par **Thi Luong DUONG**
en vue de l'obtention du diplôme de *Maîtrise ès sciences appliquées*
a été dûment accepté par le jury d'examen constitué de :

**Sofiane ACHICHE**, président
**Marek BALAZINSKI**, membre et directeur de recherche
**Xuan Tuan LE**, membre et codirecteur de recherche
**Jolanta SAPIEHA**, membre

# DEDICATION

*To my family, my director, my co-director and my friends*

# ACKNOWLEDGEMENTS

I would like to give many thanks to my supervisor Prof. Marek Balazinski, my co-director Dr. Xuan-Tuan, Le for their invaluable guidance, advice and support as well as encouraging me to complete my master's program in these two years. We are in a very touched time with the non-stop expand of Covid 19, however, they are always here to support me in any aspects of the study. It is not enough to just say thank you, but I am very grateful to be their student.

I would also like to thank for the assistance from Polytechnique Montreal, in particular, the Virtual Manufacturing Research Laboratory (LRFV) for their support; I especially want to thank Mr. Vincent Mayer and Mr. Guy Gironne for all my experimentations and collect the data analysis. Thank to Mrs. Carole Fraser for supporting me in the paper works and purchasing the stuffs for my tests needed. I give my thanks to Mr. Vincent Wuelfrath-Poirier and Philippe Plamondon at CEM lab for helping me on annealing treatment, SEM and EDX process; Prof. Myriam Brochu, Mrs. Josée Laviolette for training about the LAPOM and taking care of our test at LAPOM. And these others Polytechnique's friends that I am not able to mention here. I am glad to have met all of you and so lucky to work with you in Polytechnique.

I would like to express a deep gratitude to my family in Vietnam, my parents, my sister and my brother. They are always by my side even how far we are. They believe on my choice and encourage me in any situation.

I acknowledge the support by Natural Sciences and Engineering Research Council of Canada (NSERC) for their financial support.

Finally, I would like to spend my special appreciation to my cousin and his family. They are my family in Canada. They take care of me and give me the feeling of being with family. Thank you so much for being here with me in every beautiful time in Canada.

# RÉSUMÉ

Les composites à matrice métallique de titane (Ti-MMC) sont connus comme étant l'un des matériaux les plus difficiles à usiner. Ces difficultés sont dues à la combinaison des problèmes d'usinabilité des alliages de titane et des composites à matrice métallique (MMC). Ces composites métalliques de titane offrent des propriétés mécaniques et physiques remarquables par rapport aux alliages de titane et aux MMC. Les Ti-MMC sont ainsi très attractifs pour une large gamme d'applications dans des domaines industriels importants, tels que : l'aéronautique (structure aéronautique, moteur aéronautique…), ou l'automobile (moteur, système de freinage, arbre de transmission…). Bien qu'un certain nombre d'études sur l'usinabilité de ces matériaux aient été réalisées, les mécanismes d'usure des outils ne sont pas encore clairement compris. En particulier, la durée de vie de l'outil lors de l'usinage ainsi que la mauvaise qualité de surface obtenue après usinage.

Il a été rapporté que les mécanismes d'usure initiaux jouent un rôle clé dans la durée de vie de l'outil lors de l'usinage. En effet, le contrôle de ces mécanismes peut permettre de réguler la durée de vie de l'outil. Dans le but de changer les mécanismes d'usure initiaux, nous développons ici une nouvelle méthode pour ajuster l''usure chimique qui se produit dès les premiers moments de la coupe, par le biais d'une couche sacrificielle sur l'outil de coupe. C'est la première fois qu'un dépôt de nickel autocatalytique est appliqué sur des outils en carbure revêtus de nitrure de titane pour l'usinage.

Afin de générer une couche sacrificielle mince, nous avons développé une nouvelle technique de dépôt du nickel-bore sans courant, sur des inserts revêtus par PVD de (Ti, Al) N + TiN. Notre placage qui ne nécessite pas de prétraitement de surface repose sur un processus chimique en une seule étape, à base de diazonium. Les caractéristiques du nickel-bore révèlent que les dépôts présentent tous la même quantité de bore, 9,3 ± 0,1% en poids. Une telle homogénéité est intéressante du point de vue industriel. La couche mince sacrificielle du Ni / B est donc déposée sur les inserts revêtus de (Ti, Al) N + TiN dans des conditions difficiles mais efficaces.

En appliquant cette nouvelle méthode de placage sur les outils de coupe revêtus par PVD, un certain nombre de tests de tournage du matériau TiMMC ont été réalisés. Les conditions de coupe ont été

variées et les essais ont été réalisés avec les inserts d'origine revêtus par PVD et ceux avec la couche de placage sacrificielle de Ni / B. Tout d'abord, l'effet des conditions de coupe sur l'usure initiale a été étudiée en suivant le modèle « response surface methodology » (RSM) conformément à la conception composite centrale (CCD). Sur la base de la relation empirique et de régression, les paramètres de coupe initiaux et l'usure du flanc sont discutés. Les résultats obtenus montrent que la vitesse de coupe a un effet significatif sur les inserts d'origine et ceux avec couche sacrificielle lors du tournage des TiMMC. Cependant, à vitesse de coupe inférieure, l'usure initiale sous la couche sacrificielle augmente plus rapidement que celle pour les inserts d'origine. Afin de valider la contribution de la couche Ni / B, le mécanisme d'usure a été étudié via des analyses par SEM et AFM.

Les éléments ont réagi spontanément avec l'oxygène atmosphérique et ont oxydé le titane et l'aluminium car les conditions de travail présentent une haute pression et une température élevée. Le revêtement de nickel-bore sur l'insert a été estimé à seulement 100 nm d'épaisseur. Malgré sa minceur, ce revêtement s'est retrouvé impliqué lors du processus d'usinage dans diverses réactions thermochimiques. Dans les mêmes conditions de coupe avec les outils non revêtus, l'adhérence s'est développée lors de l'augmentation des contraintes chimiques à haute température entraînant de la diffusion. Duong et al 2016 ont rapporté que cette diffusion permet de former une couche de protection contre l'usure, permettant de protéger l'outil pendant la période d'usure régulière se produisant lors des premiers moments de l'usinage. Cependant, l'usure d'adhérence n'est plus observée lors de la première période d'usure de transition en raison de la présence du revêtement sacrificiel Ni / B. En comparaison avec les essais d'inserts d'origine, nous avons remarqué qu'avec la couche sacrificielle Ni / B, l'usure par abrasion est le mécanisme le plus important dans toutes les conditions expérimentales. Par conséquent, la présence de notre couche sacrificielle en couche mince sur l'outil de coupe a clairement changé l'usure chimique et les mécanismes d'usure qui s'opèrent lors de la première période d'usure. La couche de protection contre l'usure n'a pas été trouvée lors de la première période d'usure lors du tournage du TiMMC pour les inserts présentant la couche de placage sacrificielle. L'amélioration de la durée de vie de l'outil n'a donc pas été observée dans cette étude. L'outil revêtu de Ni / B a une durée de vie plus courte que l'outil en carbure d'origine. Le passage d'une usure par adhérence à une usure par abrasion lors des premiers instants de coupe serait le résultat de la présence de la couche sacrificielle.

Afin de mieux contrôler les mécanismes d'usure initiaux, divers matériaux de placage sont recommandés pour modifier l'activation de l’usure chimique au cours de la période d'usure initiale. Les travaux futurs s’orientent donc vers la création d’un nouveau concept de placage d'outils de coupe. Ce concept permettrait de recycler l'outillage et ainsi proposer une méthode rapide et très économique.

# ABSTRACT

Titanium metal matrix composites (Ti-MMCs) has known as one of the most difficult to machine materials due to the combination of different difficulties in machinability from both titanium alloys and metal matrix composites. These metallic composites material possess several remarkable mechanical and physical properties of both titanium alloys and metal matrix composites (MMCs). Thus, the Ti-MMCs are increasingly attractive for a range of applications in industrial areas: aerospace (Aircraft structure, aero-engine…), automotive (engine, brake system, driveshaft…). Despite various studies on the machinability of these materials have been carried out, their tool wear behaviors are still not fully understood. Furthermore, the tool life when machining the TiMMCs is very short and poor machined surface quality.

It has been reported that the initial wear mechanism plays a key role in the tool life during machining of TiMMCs, controlling the initial wear behavior can therefore solve the tool life problem. With an aim of changing the initial wear mechanism, we propose herein a simple and efficient electroless plating of a sacrificial coating nickel-boron (Ni/B) onto the cutting tool to adjust the chemical wear behavior at the first moment of cutting process. This is the first time an electroless nickel deposition has been applied to the titanium nitride coated carbide tools for a machining process.

Indeed, a thin nickel-boron sacrificial coating can be easily deposited on the existing PVD coated inserts with (Ti,Al)N+TiN. Our electroless plating relies on a one-step diazonium induced anchoring process to graft the amine-terminated groups on the inserts without requiring any surface pre-treatment. The plated surface is fully covered by a homogenous and continuous metallic film. The characterization of our obtained nickel-boron films reveals that they all contain the same amount of boron, 9.3 ± 0.1 % in weight. Such homogeneity is interesting from the industrial point of view.

In order to shed some light on the effect of our Ni-B sacrificial coating electrolessly plated onto the PVD coated cutting inserts, a number of turning tests of TiMMCs material have been conducted under different cutting conditions with both original PVD coated inserts and PVD coated inserts with a sacrificial coating of Ni/B. First of all, the effect of cutting conditions on the initial wear

was conducted by using the model of response surface methodology (RSM) in accordance with central composite design (CCD). Based on the empirical and regression relationship between the initial cutting parameters, the flank wear has been discussed. The obtained results show that cutting speed affects significantly both original and sacrificial coating inserts when turning TiMMCs. However, at the lower cutting speed, the initial wear of the sacrificial coating increases quicker than the original one. For a better understanding of the contribution of the Ni/B sacrificial coating, the wear mechanism has been further investigated through the SEM and AFM analysis.

The sacrificial coating nickel-boron on the insert has involved into the machining process and affected various thermal-chemical problem of the cutting tool. Under the same experimental cutting conditions, the adhesion wear of the pristine cutting tools is developed with an increase in chemical stresses at high temperature and therefore results in a diffusion wear. Duong et al 2016 already reported that this diffusion wear forms a wear shield layer that was considered as a protection layer for the steady wear period. However, the adhesion wear is no longer observed at the first transition wear period due to the presence of the sacrificial coating Ni/B. In comparison with the test of the original inserts, we remark that the abrasion wear is the most important mechanism under all experimental conditions in the presence of the sacrificial coating inserts. Clearly, the presence of our sacrificial coating on the cutting tool has changed the chemical wear behavior and wear mechanism at the first wear period. Since the wear shield was not formed at the first transition wear period when turning TiMMCs using our sacrificial coating, the improvement of tool life was thus not observed in this study. The observed behaviour suggests a change from the adhesion to the abrasion wear mechanism in the first period of cutting.

The primary obtained results during this thesis have opened a potential and an alternative method to control better the initial wear mechanism through a simple and efficient electroless nickel plating process. Indeed, besides Ni/B, there are various wear-resistance materials (such as Ni-P, W-P, W/Co-P, Ni-W/P…) can also be deposited onto the cutting inserts by using our eco-friendly and cost-effective plating strategy. This direction might therefore be considered in the future to get more insight into the initial wear mechanism.

# TABLE OF CONTENTS

# LIST OF TABLES

# LIST OF FIGURES

# LIST OF SYMBOLS AND ABBREVIATIONS

| | |
|---|---|
| ASB | Adiabatic Shear Band |
| AFM | Atomic force microscopy |
| ANOVA | Analysis Of Variables |
| BUE | Built-Up-Edge |
| CBN | Cubic Boron Nitride |
| CNC | Computer-Aided Manufacturing |
| CVD | Chemical Vapor Deposition |
| EDS | Energy Dispersive Spectroscopy |
| EDX | Energy Dispersive Spectroscopy |
| FIB | Focused ion beam |
| HRC | Rockwell C hardness |
| HSS | High Speed Steel |
| KT | Krater Tiefe (Crater wear) |
| MEMS/ NEMS | Micro/nano-electromechanical systems |
| MMCs | Metal matrix composites |
| PCBN | polycrystalline boron nitride |
| PCD | Polycrystalline Diamond |
| PCD | Polycrystalline diamond |

| | |
|---|---|
| PVD | Physical Vapor Deposition |
| RSM | respond surface methodology |
| SEM | Scanning Electron Microscope |
| SiC | Silicon carbide |
| SO | Sub-objectives |
| TiC | Titanium carbide |
| Ti-MMCs | Titanium metal matrix composites |
| VB | Verschleissmarken Breite (Flank wear) |
| XPS | X-ray Photoelectron Spectroscopy |

# LIST OF APPENDICES

# CHAPTER 1 INTRODUCTION

This chapter describes the basic phenomenon and major challenge when machining the TiMMCs, the current coating technologies, as well as how to solve the problems. The research questions and motivation to work on this project are then revealed. Our research objective and hypothesis are discussed to explain how the phenomenon happens. We then present our experimental plan and methodology for this project. The last section will provide the outline of the thesis.

## 1.1 Motivation and research question

Titanium alloys are widely used lightweight materials in areas due to their different adequate properties such as excellent chemical resistance, biocompatibility, and high specific strength (Hayat, Singh, He, & Cao, 2019). Additionally, they have several poor machining characteristics: the reactivity is high while the thermal conductivity and elasticity modulus are low. In particularly, their high strength and hardness are still maintained at elevated temperature (Escaich, Shi, Baron, & Balazinski, 2020; Niknam, Khettabi, & Songmene, 2014). The most important wear mechanism when machining the titanium alloys are adhesive and diffusion (Ma et al., 2020; Pramanik & Littlefair, 2015).

On the other hand, due to the abrasive properties and the reinforcement of hard particles, metal matrix composites (MMCs) have been considered as very hard to cut material. MMCs are defined by the matrix reinforcement type (Badoi & Constantinescu, 2016). Various hard particles (SiC, Al2O3, B4C, TiC, TiB2…) have been used as the reinforcement materials (Haghshenas, 2016). They were reinforced to metallic matrices through either physical or chemical method, to achieve the valuable properties of materials. MMCs reinforced with ceramic possess some advantages including but not limited to the highly specific strength, wear resistance at elevated temperature and low thermal expansion (Hayat et al., 2019). According to the hardness and physical properties of the reinforcing material, the abrasion has been found as the major wear mechanism when machining MMCs (Woon, 2021); this wear mechanism is completely different to the adhesion one when machining the titanium alloys.

Titanium metal matrix composites (Ti-MMCs) offer several remarkable mechanical and physical properties compared to standalone titanium alloys and metal matrix composites (MMCs). The beneficial characteristics from both titanium alloys and MMCs make Ti-MMCs a material of choice in important industries: aerospace (Aircraft structure, aero engine…), automotive (engine, brake system, driveshaft…). (Cao & Liang, 2020; Hayat et al., 2019). Despite these excellent properties, titanium metal matrix composites however own very poor machinability because of the high strength and hardness at elevated cutting temperatures from titanium alloys and very hard particles reinforcement and abrasive properties from MMCs. The combination of these difficulties in machinability of titanium alloys and metal matrix composite results in machining Ti-MMCs a major challenge in the field (Aramesh, 2015; X.-T. Duong, Balazinski, & Mayer, 2014).

Indeed, machining of Ti-MMCs are characterized by the complicated wear mechanism, short tool life and poor surface quality. These two factors are considered the most important criteria to improve the machinability of Ti-MMCs. (Seyed Ali Niknam, Saeid Kamalizadeh, Alireza Asgari, & Marek Balazinski, 2018; Niknam, Kouam, Songmene, & Balazinski, 2018). As a result, numbers of studies have been carried out to investigate and analyze the tool life and wear mechanism during machining TiMMCs (Cao & Liang, 2020; Mu et al., 2017; Munir, Kingshott, & Wen, 2015; Saba, Zhang, Liu, & Liu, 2019) focused on the effect of the reinforcing structure of titanium on the tool wear. Reinforcing the structure of titanium has been one of the main subjects among these studies(Cao & Liang, 2020; Mu et al., 2017; Munir et al., 2015; Saba et al., 2019). Studies on machinability of the TiMMCs (Aramesh, 2015; Bejjani, 2012) confirmed that abrasion is the most important wear mechanism during a machining process. Further investigation on the chip formation (Bejjani, Balazinski, Attia, Plamondon, & L'Éspérance, 2016) reported that the hard particles inside the matrix were found not to be hindering, or retarding the adiabatic shear bands formation. Both abrasion and adhesion are an important role when machining the TiMMCs (Bai, Roy, Sun, & Silberschmidt, 2019). By studying the tool wear at the first moment of cutting, (X. Duong, Mayer, & Balazinski, 2016) pointed out that the adhesion and diffusion are found under all tested cutting conditions within the initial wear period; while the abrasion one are found mostly in the second and third wear zone. Supporting this hypothesis, other groups (Seyed Ali Niknam, Saeid Kamalizadeh, et al., 2018; Seyed Ali Niknam, Jules Kouam, et al., 2018) proved that the adhesion and abrasion strongly impact the first wear period. More importantly, by applying the theory of

chaos, (X. T. Duong, 2015b) confirmed that tool wear evolution and tool life during machining TiMMCs depend on the initial condition and the initial wear mechanism. Therefore, changing the initial wear mechanism to handle the tool wear and tool life problem is of interested in this project.

In the mentioned research, various cutting tools were used, including Polycrystalline diamond (PCD), cubic boron nitride (CBN), uncoated and coated carbide tools. The coated carbide cutting tool is highly recommended due to the high wear rate and short tool life. In this situation, a researcher can avoid cutting a large amount of a very expensive material, like TiMMCs. In general, a coated layer consists of several outstanding features as high intrinsic hardness, chemical inert, anti-oxidation, and anti-friction. Actually, the coated tool has presented a better performance than the conventional one since it reduces friction and interactions between tool and workpiece, then decreases crescent pit wear, and hence improves tool life and cutting efficiency of the coated tool (Deng et al., 2020).

The most well-known coating methods of cutting tools are physical vapor deposition (PVD) and chemical vapor deposition (CVD) technologies. However, due to the higher deposition temperature and higher gas pressures compared to PVD of most CVD techniques, and the resulted toxicity causes pollution of environment, the application of the CVD technology is limited in the field of coating the cutting tools. Although PVD is widely used in the coated cutting tools industry (Deng et al., 2020), this technology is a complicated and costly method. It is thus important to develop new, efficient and cost-effective methods for coating the cutting tools.

Indeed, electroless plating (or chemical deposition) can be considered as an alternative to replace PVD technique for many different applications as this chemical method allows a coating on various kinds of materials (conducting and semi-conducting surfaces, oxide, and plastic). Surprisingly, only a few applications on the cutting tool were conducted. As a representative example, in the research of Aziz (Aziz et al., 2017), a ternary Ni-W-P alloy was successfully deposited onto the surface of uncoated tungsten carbide. The life of the electrolessly coated tool in this study has improved about 40% in comparison with that of the uncoated tool. The reason why electroless plating is not largely used for cutting tool industry can be explained by the fact that this technique requires a complicated pre-treatment step prior to the main plating process. Therefore, the

feasibility of the electroless plating is still questionable and an open subject for the coating of cutting tools.

Recently, we have successfully developed an eco-friendly and efficient electroless plating strategy for metalizing the surface of insulating materials: Plexiglas® (polymethylmethacrylate) (Vu et al., 2018). It is important to note that our simple plating strategy relies on a one-step diazonium induced anchoring process which provides any kinds of surface (conducting, semi-conducting or insulating surfaces) with amine-terminated groups. Once the surface is aminated, an electroless plating of nickel-boron can be easily carried out in open air and at moderated temperature. As a result, such the cost-effective electroless plating strategy is being explored in the domain of micro/nano-electromechanical systems (MEMS/NEMS). It is thus interesting to extend the application of our electroless nickel plating to the other materials such as the cutting tool ones. On account of these factors, we are motivating to focus our attention on ceramic surfaces (ex. $Si_3N_4$, TiN, TiCN…) which are standout materials particularly for micro-nano fabrication but also for wear resistance applications.

As clearly indicated above, developing a novel method to plate an additional sacrificial coating onto the existing coated tools to adjust initial wear mechanism when machining the TiMMCs is an exciting topic. All the anticipated problems leave open some original questions as follows:

1. **How to change the initial wear mechanism when turning TiMMCs material?** In the case where the initial wear is adjustable, we may be able to predict the tool wear evolution over time and the tool life as well. More importantly, if we can control the initial wear mechanism through the formation of a wear shield layer at the first transition period, we will be able to improve the tool life.
2. With the aim of changing the initial wear mechanism at the first moment of cutting, plating an additional thin layer onto layer onto an the PVD coated inserts is proposed. This thin film will be considered as a sacrificial coating that will be involved into the machining process by means of chemical reactions with the workpiece and tool material and consequently this film contributes to change the wear mechanism. So, the question is: **Is it possible to apply an electroless deposition method to plate a sacrificial coating onto an existing PVD coated insert**?

3. The last question dealing with the tool life prediction. When the two first questions given above have been addressed, how we can apply this method to improve the tool life during machining of TiMMCs?

## 1.2 Hypothesis

Based on the research problem and questions, the following hypothesis statements will be utilized in this work:

- The sacrificial coating of Ni/B is successfully coated on the surface of the PVD coated inserts, and the sacrificial coating has the best hardness.
- The electroless plating method will modify the cutting tool surface without altering its intrinsic properties of the substrate materials.
- By coating a sacrificial coating of condensed and continuous film Ni/B onto the coated one (Ti,Al)N + TiN, we expect that the initial wear mechanism will change, and the tool life is thus improved.

## 1.3 Research objectives

By developing a new efficient coating method on carbide coated ((Ti,Al)N + TiN) cutting tool, the main objective of this study is to create a sacrificial coating to adjust the initial wear mechaniam during a machining of TiMMCs. The initial cutting conditions and initial wear mechanism are reported to be effected significantly the tool life; our specific objectives are thus given here below:

- Develop an electroless nickel plating method to plate a sacrificial coating onto the existing coated carbide insert with ((Ti,Al)N + TiN).
- Determine the influence of cutting conditions on the tool wear during machining of TiMMCs based on the response surface methodology (RSM).
- Characterize the effect of sacrificial coating on the tool wear mechanism during turning TiMMCs.

## 1.4 Research approach

In order to complete the objectives of the research, we use numerous measurement tools and equipment. Along with those, various analysis methodologies were applied in this study. Our methodology to follows within the framework of this project as given in Figure 1-1.

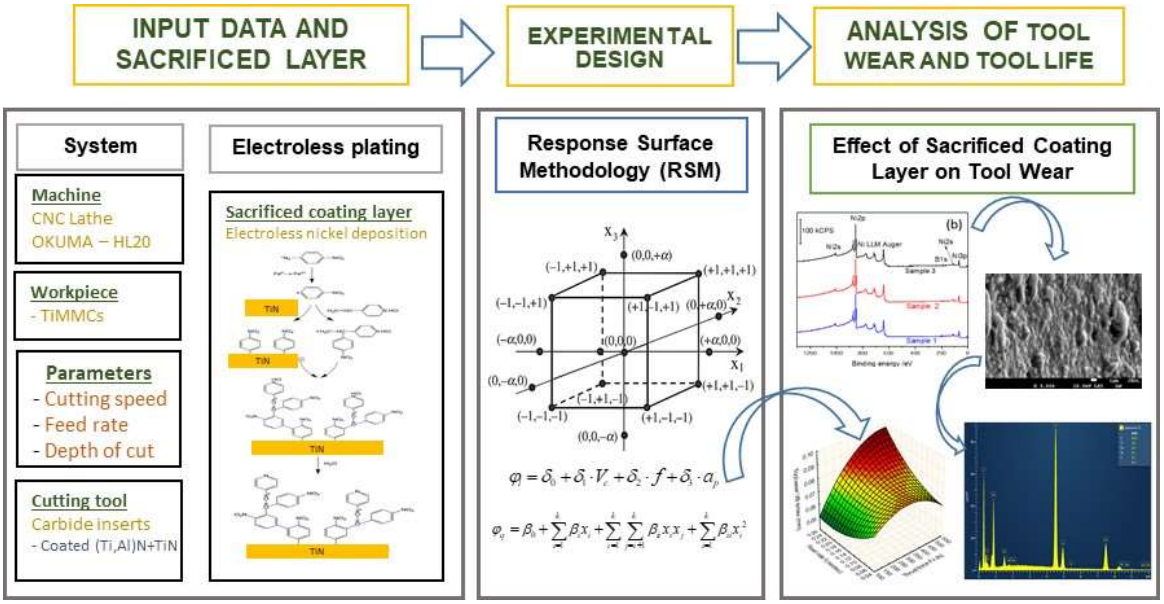


Figure 1-1. Methodology to be followed

Electroless nickel plating: Series chemical experiments with two main steps to make the sacrificial coating for the tools: (1) grafting of amine-terminated seed layer by **diazonium** induced anchoring process, (2) **electroless plating** on tools process. X-ray photoelectron spectroscopy **(XPS)** and Atomic force microscopy **(AFM)** are carried out to elucidate the mechanism of surface functionalization as well as the activation of the grafted layer. These methods allow us to achieve the first sub-objective.

The electroless plating film is characterized by means of **SEM, EDX** & XPS techniques. These techniques allow confirming the feasibility of our electroless plating strategy and measuring the composition of the obtained Ni-B alloy.

We design the turning experiments by response surface methodology **(RSM)** & **tool life investigation** models (1). Conducting the machining processes on the CNC Lathe OKUMA –

HL20 machine in the Polytechnique's laboratory with Ti-MMCs material (2). Measure tool wear by counting the pixels in the captured photos with **Canon EOS 300D camera** (3).

Analyze the initial tool wear mechanism using **ANOVA**, scanning electron microscope **(SEM)** followed by Energy Dispersive X-Ray **(EDX)**, which is commonly used to exhibit the chemical structure or crystalline composition of a material.

## 1.5 Outline of the thesis

Chapter 2 deals with a background knowledge of the machinability of titanium metal matrix composites. It also provides the literature review of tool wear and tool life during turning TiMMC with different types of cutting tools. Especially, this chapter mentions the applications of a new approach coating method – i.e., electroless nickel deposition.

Chapter 3 describes the entire experiment process from sample preparation, test designation, and methodologies used in this study.

Chapter 4 summarizes the first publication of our research group related to electroless deposition of Ni-B onto ceramic materials. The main part of this chapter presents a successful deposition of Ni/B onto the surface of coated ((Ti,Al)N + TiN) cutting tool. We also characterize the sacrificial coating to determine the chemical composition of the Ni/B layer.

Chapter 5 analyzes the flank wear results, and initial wear mechanism of electroless Ni-B coated cutting tool during turning Ti-MMCs. The effect of the sacrificial coating on the tool wear mechanism will be also characterized in this chapter.

Chapter 6 is the general discussion and conclusion of this study. The scientific distribution of this research and some recommendations for the future work are proposed in this chapter.

# CHAPTER 2 LITERATURE REVIEW

## 2.1 Machinability of Titanium Metal Matrix Composites (TiMMCs)

Following the statistical data in the research of Carl J. Nicholls (Nicholls, Boswell, Davies, & Islam, 2017), numbers of studies on machinability of metal matrix composites (MMCs) have been developed since the early 1970s. The MMCs have been widely used in the industries of aerospace and automobile since the 1980s. At present, due to the outstanding characteristics, MMCs solved a lot of problems and demonstrated various industrial applications that were not offered before by conventional monolithic materials. They are also used in several other fields such as biomechanics or ground transportation or transport structures…("16 - Metal matrix, fibre–metal and ceramic matrix composites for aerospace applications," 2012; Fan & Njuguna, 2016; Mallick, 2012). MMCs have resulted from the presence of two or more distinct phases.

Titanium alloys are lightweight materials. They have attractive properties such as excellent chemical resistance and biocompatibility, and high specific strength (Hayat et al., 2019). In contrary, they are characterized by several poor machineabilities such as high reactivity, low thermal conductivity, and low elasticity modulus. The high strength and hardness of titanium alloys are maintained at elevated temperatures. (Niknam et al., 2014).

Because of the challenge in machining, the closed net-shape of the product is then produced to minimize the manufacturing time. We here present a “schematic of CHIP (Cold and Hot Isostatic Pressing) process for the production of near-net-shape” in (Aramesh, 2015).

A process of CHIP includes bending raw materials, pressing bender materials in CIP (Cold Isostatic Pressing) to be compacted materials, forming the alloy or MMC in sinter under high temperature via low pressure, producing final products through three ways (Hot Isostatic Pressing (HIP): to enhanced properties of materials, extruder or forge) Figure 2-1.

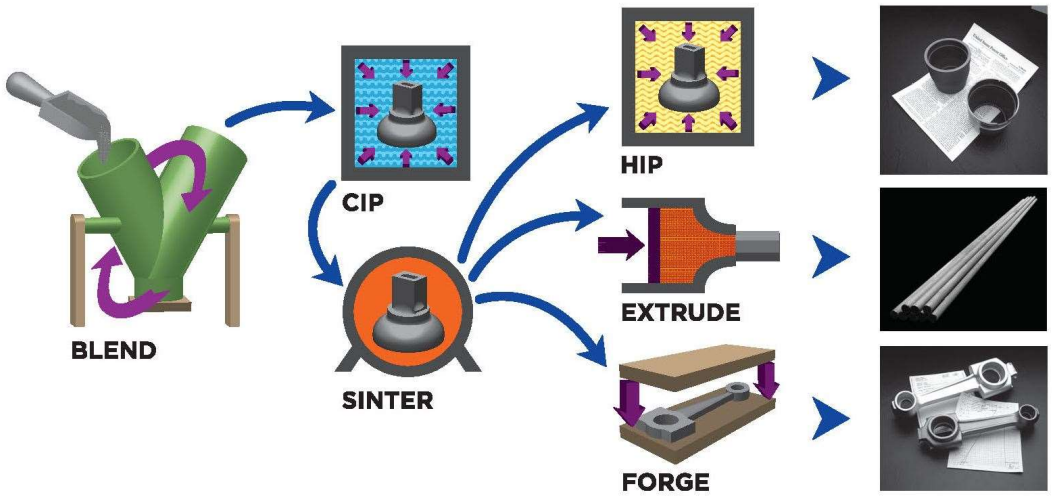


Figure 2-1. Schematic of CHIP process for the production of near-net-shape products (reproduced of (Kamali Zadeh, 2016))

After a production to close to the final shape, a finish machining of Ti-MMCs is needed to achieve the acceptable surface quality before transferring to the cutting process. However, the poor machinability will cause a high rate of tool wear, a short lifetime of the tool, and poor surface finishing. Thus, they are the most major disadvantages during machining Ti-MMCs.

## 2.2 Cutting tool during turning TiMMC

An ideal cutting tool is expected to consist of the characteristics of high hardness, good toughness, and wear resistance (Astakhov, 2013; Byrne et al., 2003) (Astakhov, 2013; Byrne, Dornfeld, & Denkena, 2003).

The hardness of the tool material is defined as the ability to resist the hard of the workpiece. It is relevant to the material strength and evaluates the level of the deformation resistance. The ability to retain the high hardness of material at high temperature is the definition of hot hardness. Therefore, the hot hardness is one of the most important features of the cutting tool (Astakhov, 2013)(Astakhov, 2013). Nowadays, the hardest tools used in metal machining are Polycrystalline diamond (PCD) and cubic boron nitride (CBN). Figure 2-1 shows the corresponded hardness of typical tool materials over temperature.

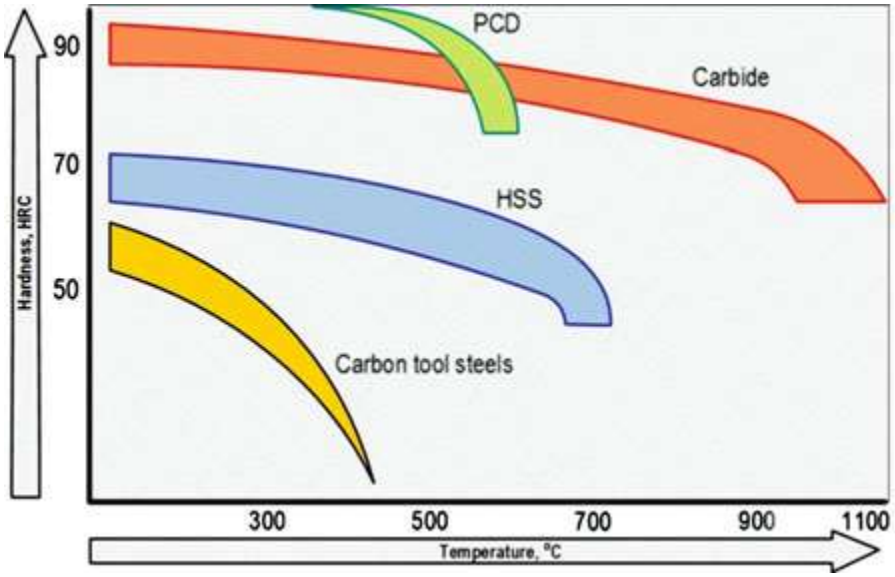


Figure 2-2. Hardness of tool materials versus temperature. (Astakhov, 2013)

The definition of toughness is referred as the ability of tool material to absorb energy before fracture (Astakhov, 2013). Toughness is correlative to numerous crucial properties of cutting materials such as vibration and shock-load resistance.

Materials with both hardness and toughness are well suited to industrial cutting tools (Heath, 2001).

High hardness is a requirement for industrial machining. Without toughness, however, cutting tools wear frequently. To circumvent this problem, the hard material is coated on the tough core. The resulted cutting tools gain both wear resistance and high fracture toughness. (Dobrzański & Dołżańska, 2010).

Wear resistance of cutting tools is determined as the ability in attaining its high reliability before replacement (Astakhov, 2013). Hung et al. found that the wear resistance of polycrystalline boron nitride (PCBN) and Polycrystalline diamond (PCD) is better compared to WC inserts (Hung et al., 1996).

In order to balance a combination of the expected characteristics for the desired tool, various tool materials have been tested. Heath highly recommended PCD tools for machining MMCs because its dominant wear mechanism is abrasive wear (Heath, 2001). Furthermore, in the literature on Ti-MMCs machining, PCD tools are also preferred over carbide tools due to longer tool life and higher surface roughness quality (Bejjani, 2012; Bhushan, Kumar, & Das, 2010).

Another alternative cutting material is cubic boron nitride (CBN), which is the second hardest cutting material after PCD. Despite its lack of toughness, CBN has high hot hardness at up to 1,500° C and great wear resistance (Hosseini & Kishawy, 2019).

The high cost of PCD and CBN tools requires identifying other cost-effective alternatives such as coated carbides (TiAlN/TiN-coated, triple-layer TiC/$Al_2O_3$/TiCN-coated) and even uncoated carbide (Davim, 2008).

As an alternative solution for PCB or CBN tools in lower cutting conditions requirement, the carbide tool was the first presented by the researchers in Germany as a new tool in 1927 (Kamali Zadeh, 2016). In the next section, a literature review on their applications in machining Ti-MMCs will be provided.

## 2.3 Literature study about the machining of titanium metal matrix composites using carbide tools.

In the research of Aramesh (Aramesh, 2015), the primary wear mechanism of CBN and carbide tools is adhesion, flow by abrasion, and diffusion.

Duong X.T et al. (X. Duong et al., 2016) reported that the initial tool wear mechanism has a significant effect on the entire tool life during machining TiMMCs. Therein, during the transition from the initial wear region to the steady wear one, a protective layer, so-called “wear shield”, is formed through an adhesion of workpiece material on the tool wear surface. The adhesion and diffusion are also found as the major wear mechanism in the initial tool wear, while abrasion wear is less apparent. Additional information on initial tool wear can be found in (Kamali Zadeh, 2016).

(Seyed Ali Niknam, Saeid Kamalizadeh, et al., 2018) investigated the turning process of Ti-MMCs with carbide and CBN inserts under various cutting conditions. The authors found that the typical wear modes observed in the carbide inserts were abrasion and adhesion.

## 2.4 Tool wear and tool life in machining TiMMC

Cutting conditions, types of tools, materials of the workpiece, machine tools e.g. are the effected factors on the tool wear.

As the result, the tool wear has been observed in different mechanisms during the metal machining. Because of the presence of various mechanism, the tool wear is really complicated.

When machining at very high cutting speeds, tool geometry can be damaged by creep and oxidation. The creep can cause a characteristic of a rear bead in the zone of maximum temperatures. The tool can oxidize in ambient air at high temperatures, especially in well-ventilated areas near the cutting one. These two mechanisms, creep and oxidation, increase with cutting speed.

There are several different types of tool wear are shown in the Figure 2-3. They are: (a) flank wear;(b) crater wear; (c) notch wear; (d) nose radius wear; (e) comb (thermal) cracks; (f) parallel (mechanical) cracks; (g) built-up edge; (h) gross plastic deformation; (i) edge chipping or frittering; (j) chip hammering; (k) gross fracture. (Stephenson & Agapiou, 2016)

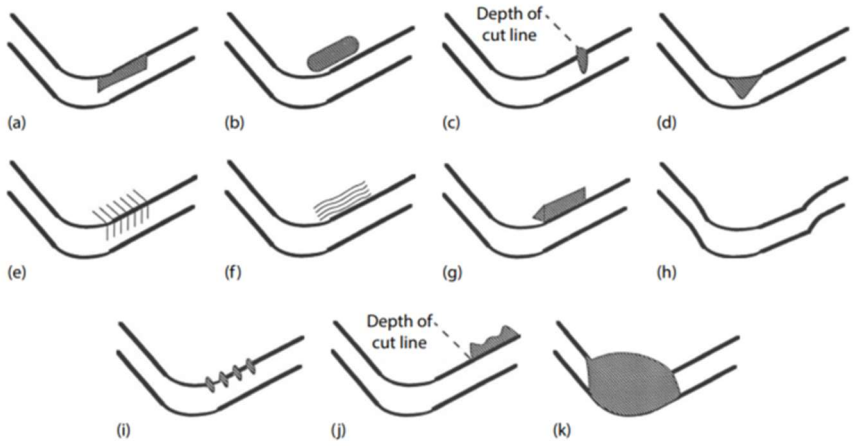


Figure 2-3. Types of wear on cutting tools (Stephenson & Agapiou, 2016)

In this present work, we mainly focus on the flank wear (Figure 2-3 (a)). Other types of wear, such as notch wear, built-up edge (BUE) Figure 2-3 (c & g) will be also investigated in this study.

## 2.5 Physical vapor deposition (PVD) coatings

Due to the appearance of various difficult to machine materials, PVD in term of deposition hard coatings onto cutting tool has been paid more attention in the recent decades. PVD is considered one of the most used coating methods for cutting tools currently. PVD technology is widely applied in the coated cutting tools industry (Deng et al., 2020).

Hereunder presents some common coated materials:

**Titanium Carbide (TiC):** It is the most used carbon coating. In general, a layer of 5 microns is deposited on the base metal. Several grades of TiC are available. Adding a layer of TiC has several effects: reducing the length of contact between the wafer and the chip; the friction reduction in the cutting area and thereby reducing the cutting force; increasing the wear resistance.

**Aluminum oxide ($Al_2O_3$):** Aluminum oxide is used in single-ply and multi-layer pads. In the first case, a layer of 5-micron coated substrate a special sintered carbide, while in the latter, an aluminum oxide layer overlies a layer of TiC.

**Titanium nitride (TiN):** this coating layer has a gold color. It performs a high wear resistance via various cutting materials. The finished surface quality and tool life have a significant improvement when using this coated tool. Titanium nitride does not have the same hardness as TiC and Al2O3, but it lowers the coefficient of friction on the cutting face and improves resistance to crater wear. It uses less substrate and can be applied to cutting tools at a lower temperature than TiC and Al2O3.

**Titanium aluminum nitride ((Ti, Al) N):** The color of this coating is purple/black color. Its super oxidation resistance lead the coated tool to be an excellent option for interrupted operations (Astakhov & Davim, 2008)

**Multilayer coating layers:** The application of different layers, one over the other can tap the best properties of each material used in its composition. The total thickness of the layers does not exceed generally 2 to 12 microns. The wear resistance generally increases with the thickness of the coating, but it simultaneously increases the fragility and tendency to chipping. In comparison with the single-layer, the multilayer coating (TiC/Al2O3/TiN) or (Ti,Al)N+TiN is more efficient than a single-ply coating of TiC or TiN. Figure 2-4 shows a schematic of the multilayers of PVD coating.

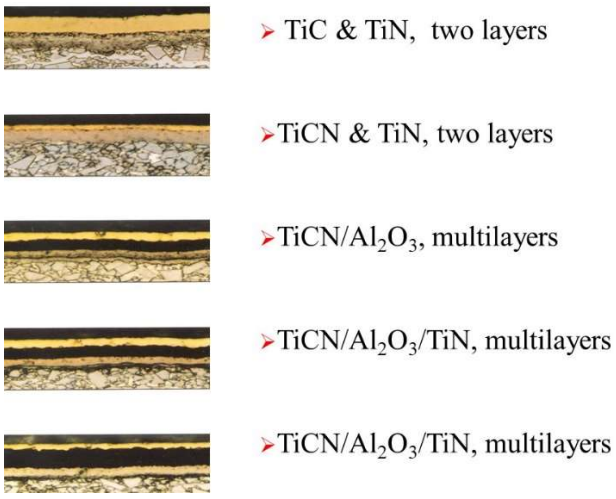


Figure 2-4. Multilayers of PVD coating (refer to the lecture of course code: MEC8554 in Polytechnique of Montreal)

With a purpose of improving the machined surface quality by self-lubrication of the tool, a soft and lubricious materials Al-Si were deposited through either the conventional PVD or the proposed pre-machining method. These two methods were compared in machinability in machining Inconel 718. The results showed that both of them contribute significantly to the surface integrity of the machined surface (Montazeri, Aramesh, & Veldhuis, 2020).

However, PVD is a costly and complicated method while pre-machining cannot control the thickness of the coating layer. Hereafter, we present a novel coating method which is applied on a TiN-coated tool for the first time to the best of our knowledge.

## 2.6 Nickel electroless plating and applications.

In the field of surface coating, electrodeposition is a well-implemented technology due to its relatively easy installation and high performance. This technique is either galvanic-induced (electroplating or more precisely electrolytic plating) or self-catalytic processes (electroless). The electroless process displays lower deposition rates than electroplating. However, the coating by electroless presents larger homogeneity than electrodeposited films since electroless is a non-electrical process. (Fuentes, 2010). In the scope of the thesis, we focus on the electroless deposition technique.

Recently, electroless deposition has been considered a universal method in material surface treatment. Unlike electroplating which works with only conducting and semi-conducting surfaces, electroless plating can be applied to various kinds of materials (conducting and semi-conducting surfaces, oxide, and plastic). In the term of metalizing the insulating substrates in MEMS field, (Zeb, Duong, et al., 2017) presented a successful electroless nickel plating on the surface of KMPR epoxy photoresist polymer. (Vu et al., 2018) reported a one-step process of covalent grafting of vinylpyridine groups on the surface of commercial Plexiglas® (polymethylmethacrylate) employing diazonium-based aqueous chemistry, without requiring any surface pre-treatment step.

An application of the diazonium-induced anchoring process in the fabrication of microelectromechanical systems has been carried out in the study of (Zeb, Zafar, Palacin, & Le, 2017).

Although it has many advantages on the various material surface as mentioned but only a few applications on cutting tools were conducted. In the research of Aziz (Aziz et al., 2017), a ternary Ni-W-P alloy was successfully deposited onto the surface of uncoated tungsten carbide. The life of the electroless coated tool in this study has improved 40% compared to the uncoated tool. However, a pre-heat treatment for the tool surface is required prior to the plating process.

Due to the challenges in the pre-treatment steps, electroless deposition technology is still a questionable and open subject in coating the cutting tools.

Our research group has successfully developed the electroless deposition method in metalizing the surface of insulating materials: KMPR photoresist polymer (Zeb, Duong, et al., 2017) or Plexiglas® (polymethylmethacrylate) (Vu et al., 2018). These materials are widely using in the domain of micro/nano-electromechanical systems (MEMS/ NEMS). It is thus interesting to extend the application of that electroless nickel plating process to the other materials. The cutting tool materials can be given here as a representative example.

## 2.7 Conclusion of the literature review

Titanium metal matrix composites have very poor machinability due to their hard and abrasive ceramic particles within the matrix structure. Furthermore, they are expensive and non-recyclable

materials. As an evidence, the poor tool finished surface, high tool wear, and short tool life are the main problems in machining Ti-MMCs.

The coated tool has been proved to have super performance in machining compared with the uncoated tool. However, the current coating method PVD has some limitation in a complicated process, and high production cost. Developing new coating methods with highly efficient, friendly, and cost-effective is of interest within our research group.

Electroless deposition has advantages in material surface treatment due to the application of various materials and industrial fields. But its pre-treatment process makes it less applicable in the field of the cutting tool and wear resistance.

We here proposed a novel approach of electroless nickel deposition onto our carbide coated cutting tool with an objective of increasing tool life through a sacrifice coating layer for the tool.

# CHAPTER 3 EXPERIMENTAL SECTION

In this project, the experiments were divided into two parts: electroless plating part and machining experiment part. The first electroless plating process was mainly realized in our industrial partner's laboratories (C2MI, Bromont (QC) and PCAS Canada, St-Jean sur Richelieu (QC). Some of the tests were performed in the chemical laboratory of the Department of Mechanical Engineering (Polytechnique Montréal). These inserts were then applied on the first phase of the machining experiment which will be presented in the machining experiment part. The second process of electroless plating was carried out a part in LABPOM in Polytechnique Montreal. After plating, all these inserts were annealed in the Centre for Characterization and Microscopy of Materials (CM)2 in the required conditions. The machining experiments are all implemented at the virtual manufacturing research laboratory (LRFV) in Polytechnique Montreal. The machining parameters and conditions were selected referenced the previous studies in the same researched domain (X. Duong et al., 2016; Kamali Zadeh, 2016).

## 3.1 Samples preparation

Low Pressure Chemical Vapour Deposition (LPCVD) silicon nitride layers were deposited on 200 mm diameter $SiO_2$/Si wafer (100) on a SPTS/AVP-8200 tool using dichlorosilane and ammonia gases. The process was optimized to obtain about 480 nm thick nitride layer at a deposition rate of 1.5 nm/min. Laboratory scale samples (coupons) were prepared using a diamond-tipped cutter. These samples were successively cleaned in isopropanol, acetone, ethanol, and deionized water in an ultrasonic bath (Cole Parmer, model 08895-91) for a cumulative duration of 30 min, and they were then dried with a nitrogen stream.

The samples for these experiments are the carbide inserts grade of TS2000 with PVD coated by (Ti,Al)N+TiN for turning, which were purchased from OUTILS DE COUPE DRILLMEX INC. (Insert style: CNMG, insert size: 432, chip breaker type: MF4). Some other specifications of the insert are described in Table 1.

Table 1. Main characteristics of the CNMG 432-MF4 TS200 insert

| Name | D1 | EPSR | IC | Schematics |
|---|---|---|---|---|
| Description | fixing hole diameter | insert included angle | inscribed circle diameter | 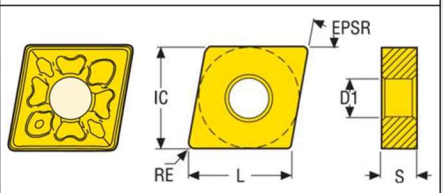 |
| Value | 0.203 in | 80.000 deg | 0.500 in | |
| Name | L | RE | S | |
| Description | Theoretical cutting edge length | corner radius | Insert thickness | |
| Value | 0.508 in | 0.031 in | 0.187 in | |



## 3.2 Electroless nickel plating onto lab-scale silicon nitride ceramic and carbide inserts through the diazonium induced anchoring process.

The direct grafting of aminophenyl layer on as-deposited silicon nitride substrates was performed at room temperature in open atmosphere without any pre-treatment by using the diazonium induced anchoring process (DIAP). To prepare 0.04 M aminophenyl diazonium salt solution, 1.08 g of para-phenylenediamine (ACS reagent 99%, Sigma Aldrich) was first dissolved in 250 mL of 0.25M hydrochloric acid solution and then 0.69 g of sodium nitrite (ACS reagent ≥97.0%, Sigma Aldrich) was added and stirred until a homogeneous solution was obtained. An amount of 0.5 g iron powder (Alfa Aesar) was added to the solution. After adding Fe powder, all samples were immediately immersed in the beakers. The experiments were carried out in the absence of stirring and in the dark to avoid UV light during grafting. The samples were taken out of the solution after 120 min. The modified samples were sonicated successively in deionized water and isopropanol alcohol for 10 min each. A nitrogen gun was used to dry all the samples. Further information concerning our DIAP process for direct amination of any surface (conducting and semi-conducting surfaces, oxides, plastics, ceramics) can be found in our recently published works (Vu et al., 2018; Zeb, Duong, Balazinski, & Le, 2020).

That DIAP process was therefore considered to graft covalently vinylpyridine groups onto the inserts as already described in detail in our previous work (Vu et al., 2018). First of all, the as-received inserts were successively cleaned in acetone, isopropanol and water under sonicated condition (5 mins/each). In parallel with the cleaning process, 250 mL of acidic diazonium solution containing 0.5 M HCl, 0.005 M 4-nitrobenzenediazonium tetrafluoroborate and 0.05 M 4-vinylpyridine was prepared. 0.2 g Fe powder (10 µm, Alfa Aesar) was then put into this solution.

Once the solution was bubbled after adding iron powder, all inserts samples were immediately immersed in the solution. The grafting was carried-out in the dark without stirring. After an immersion of two hours, the samples were washed with HCl (0.5 M), deionized water and isopropanol under ultrasonic condition. These aminated samples were dried using nitrogen gas.

After grafting the amine-terminated groups on the silicon nitride ceramic and the carbide inserts, these modified samples were were activated by simply immersing in $PdCl_2$ (10 μM)/HCl (0.5 M) solution at room temperature for 5 minutes. Afterwards, the activated samples were rinsed by deionized water under ultrasonication to remove physically sorbed palladium cations on the sample surfaces. The electroless nickel plating was performed in an ultrasonic bath (Cole Parmer, model 08895–91) at 65 °C (please see the supporting information 1). This supported video provides our entire plating processes. The plating bath consists of 0.1 M $NiSO_4.6(H_2O)$, 0.2 M citric acid monohydrate, 0.05 M dimethylamine borane (DMAB). The pH of the bath was adjusted to 9-10 using tetramethylammonium hydroxide (TMAH). For the silicon nitride samples, electroless plating time was carried out during 6 minutes while an immersion time of 30 minutes was applied to the insert samples.


a) fume-hood b) hot-plate and chemical bath in a beaker c) digital pictures showing the inserts before and after plating

Figure 3-1. An example of an electroless nickel plating setup consisting of (a) fume-hood, b) hot-plate and chemical bath in a beaker, c) digital pictures showing the inserts before and after plating

*Link: Video of nickel electroless plating process*

After the electroless nickel plating, all inserts were annealed. The process is to preheat the tube furnace to 250°C under a constant flow of $N_2$ gas. When the temperature is stabilized, the samples will be inserted into the furnace and leave them there for 30 minutes. After 30 minutes, the samples will be pushed out on the other end of the tube furnace so they can cool to room temperature under the protective $N_2$ atmosphere. The steps of annealing as following:

- Fill the alumina boat with samples (about 8-10 samples).

- Start the furnace at the annealing temperature.

- Wait until the temperature is stable.

- Start the protective gas flow (nitrogen).

- Insert the alumina boat in the heat zone of the furnace.

- Anneal the samples for the required duration.

- Push the alumina boat out of the furnace (another end of the tube).

- Let the samples cool down to room temperature under the protective gas atmosphere (10 minutes).

- Stop the protective gas and remove the samples from the tube.

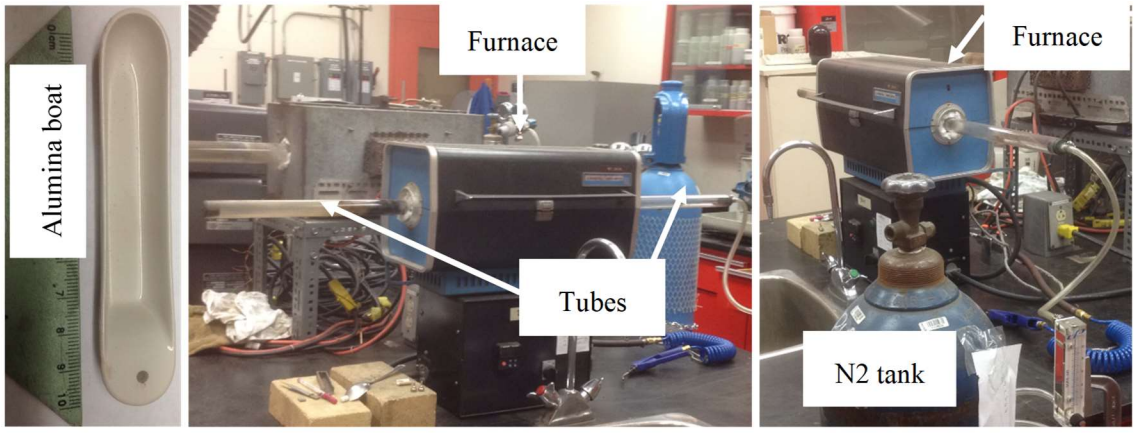


Figure 3-2. Annealing equipment

## 3.3 Scanning electron microscopy (SEM) and Atomic force microscopy (AFM)

Scanning electron micrographs of pristine and nickel-deposited samples were performed with a Hitachi SU3500 operating at 10 kV in secondary electron imaging mode. The setup was also equipped with energy dispersive X-ray detection system. AFM images were recorded on the surface of 1 $\mu m^2$ using Pico SPM LE (Agilent Technologies/Molecular Imaging) at a scan velocity of 0.5 μm/s.

## 3.4 X-ray photoelectron spectroscopy (XPS) and energy dispersive spectroscopy (EDS)

XPS survey (scan rate of 1 eV) and high-level core (scan rate of 0.1 eV) spectra were recorded using an X-ray photoelectron spectrometer (K-Alpha, Thermo Scientific) which is equipped with a micro-focused Al Kα X-ray source (1486.6 eV). The electron takeoff angle was set at 90° during data acquisition. Charge neutralization gun was used to avoid any surface charge build-up during X-ray scans. Peak-fitting procedures were performed using the software CasaXPS (version 2.3.16).

EDS spectra were obtained with two SEM (Jeol, JSM -840A and Jeol JSM 7800F FEGSEM) equipped with an Oxford X-ray detection system (AZtec EDS) for elemental analysis and quantitative mapping was used. Moreover, Joel JSM is a field emission SEM equipped with field emission guns (FEG) which provides the extreme resolution of 0.8 nm at 15 kV and 1.2 nm at 1 kV. The micrographs of the microstructures were captured at a low magnification and at a high magnification.

## 3.5 Machining TiMMCs

### 3.5.1 Experiment set up.

The turning tests were conducted under the dry condition on the CNC Lathe OKUMA – HL20. The workpiece was a piece of 394 mm length of Ti-MMCs with a diameter is 103.5 mm. The chemical and mechanical composites are shown in table 1 and table 2:

Table 2. Chemical composites of Ti-MMCs (S. A. Niknam, S. Kamalizadeh, A. Asgari, & M. Balazinski, 2018)

| Chemical analysis of Ti-MMCs | Aluminum (Al) | Vanadium (V) | Carbon (C) | Oxygen (O) | Iron (Fe) | Nitrogen (N) | Hydrogen (H) | Titanium (Ti) |
|---|---|---|---|---|---|---|---|---|
| Mass % | 5.55 | 3.84 | 0.97 | 0.26 | 0.004 | 0.21 | <0.003 | Remainder (89.163) |

Table 3. Mechanical properties of Ti-MMCs (Kamali Zadeh, 2016)

| Material | Yield strength (MPa) | Tensile strength (Mpa) | Elastic Modulus (Gpa) | Shear Modulus (MPa) | Fracture toughness (MPa/m1/2) |
|---|---|---|---|---|---|
| Ti-MMCs | 1014 | 1082 | 135 | 51.7 | 40 |

In these experiments, the nickel-boron plated carbide inserts TS2000 ((Ti,Al)N + TiN) and the carbide inserts TS2000 ((Ti,Al)N+TiN); which manufactured by SECO, were used. The specification of the cutting tool as follows: rake angle: $\gamma_0$=6°, clearance angle: $\alpha$= 0°, nose radius: $r_\varepsilon$= 0.4 mm and included angle: $\varepsilon_r$= 80°, setting cutting edge angle $K_r$= 95°, inclination angle $\lambda_s$= 6°. Cutting tool, the workpiece was set up on machine tool in the manufacturing research laboratory (Polytechnique de Montreal) as Figure 3-3.

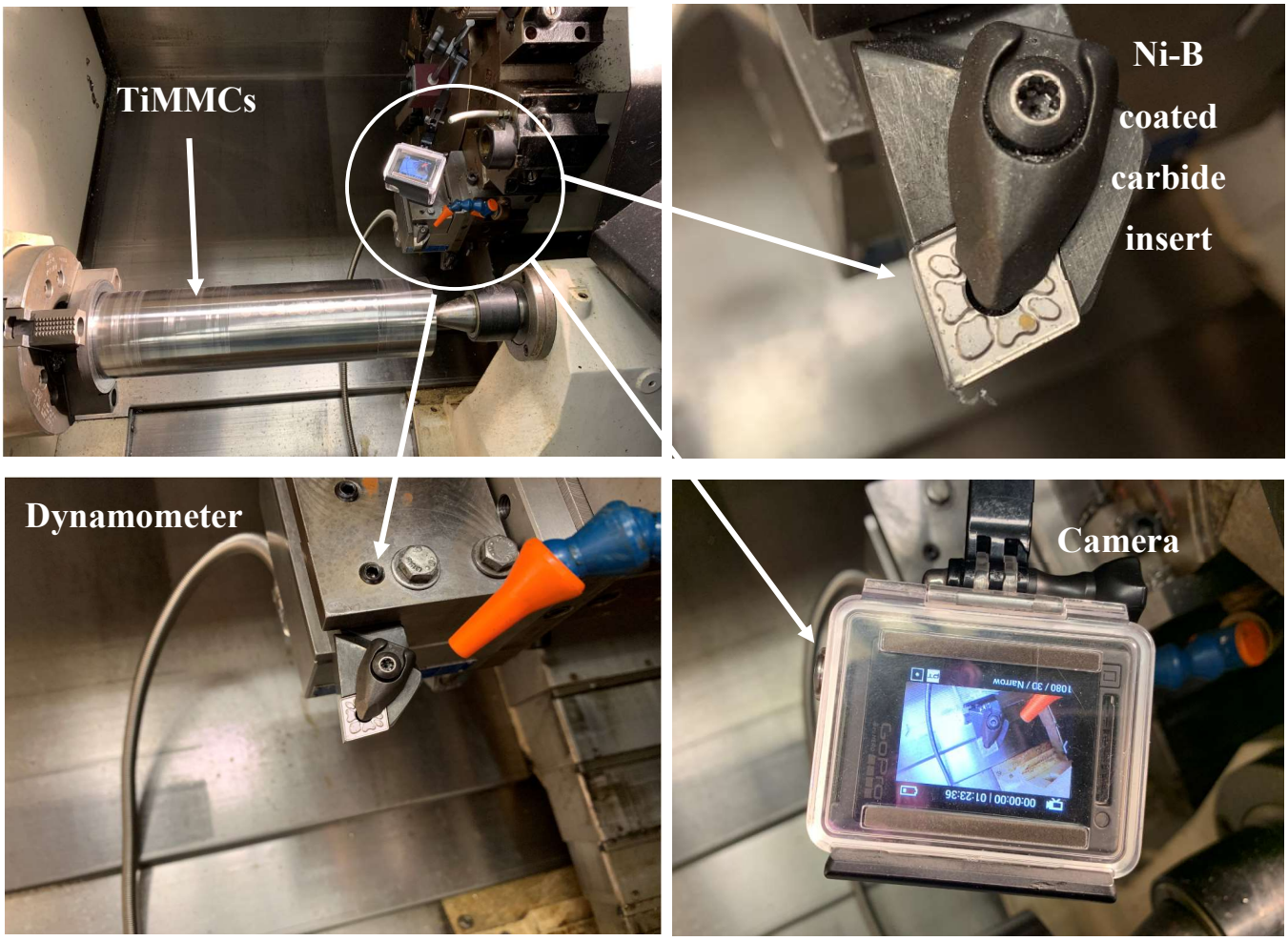


Figure 3-3. Experiment set up in the manufacturing research laboratory (Polytechnique de Montreal)

### 3.5.2 Turning experiment model I

In order to investigate the effect of the sacrificed layer (Ni-B) onto the cutting tools during machining of TiMMCs, response surface methodology (RSM) was employed for modeling and analyzing the machining parameters as cutting speed, feed rate, depth of cut on the response factor: tool wear (average flank wear VBB in this case).

To optimize the number of the machining test and evaluate the effects of certain factors on some specific results; and to quantify the effects of one or more input variables on the response factors as well, the number of experiments were defined based on the central composite design (CCD)

method, the matrix design for $k$ factor experiment is defined through the level of independent variables and the number of the experiment as hereunder Eq. (1): $n = 2^k + 2k + n_0$ (1)

Where $2^k$ is the number of experiments in factorial design; 2k are experiments in star design and $n_0$ is the number of central points. In current experimentation, three experimental factors and six central points have led to twenty of the total runs are considered. The level of independent variables for CCD are modeled as summarized in Table 1; the lowest and highest values are calculated through the scaled parameter (α) which depends on the experiment factor number considered through the relation of formula $\alpha = (2^k)^{1/4}$; with the three mentioned factors, the value of α is obtained: α=1.68179.

Table 4. Level of independent variables for CCD

| Levels | Lowest | Low | Medium | High | Highest |
|---|---|---|---|---|---|
| Coding | (-α) | (-1) | 0 | (+1) | (+α) |
| Cutting speed (Vc) (m/min) | 19.77 | 30 | 45 | 60 | 70.23 |
| Feed rate (f) (mm/rev) | 0.07 | 0.1 | 0.15 | 0.2 | 0.23 |
| Depth of cut (ap) (mm) | 0.66 | 1 | 1.5 | 2 | 2.34 |

### 3.5.3 Turning experiment model II

In order to determine precisely the lifetime of the cutting tool, numerous turning tests were performed under the condition of dry cutting with a constant depth of cut (ap = 1 mm) and feed rate (fr = 0.15 mm/rev), three-level of cutting speed (Vc = 20, 40, 60 rev/min). Each cutting speed was carried out with several intervals of cutting time from 1s to 90s. The flank wear of each edge of inserts was then measured by counting pixels in the captured photos. An analysis of cutting tool wear was implemented by taking into account the flank wear values, wear rates, and the observed flank wear curves.

### 3.5.4 Tool wear measurement method

The tests were implemented orderly and started with a new angle of the insert. After finishing each test, the insert was removed carefully and put orderly into the remarked boxes waiting for measuring the flank wear. The tool wears then were measured by counting the pixels in the captured photos with a high-resolution camera (Canon EOS 300D) (Figure 3-4).

Figure 3-4. Measuring of VBB by Canon digital camera

To measure VBB, first, the worn-out length (b) was measured using the Irfan view tool to count the pixels. Then, near zone N whose length is equal to b/4, VBB was measured. VBB is the distance between the rake face plane and the end of the worn-out region. In order to have a precise measurement, at first, a photo of all worn out flank faces was taken with the camera and then, VBB in the photos was measured by counting the pixels. To have the same conversion factor in all photos, the camera was fixed at the same distance from the inserts and with the same zoom setting.

Also, for each insert in the same place in the picture as well (in the center to avoid distortion)

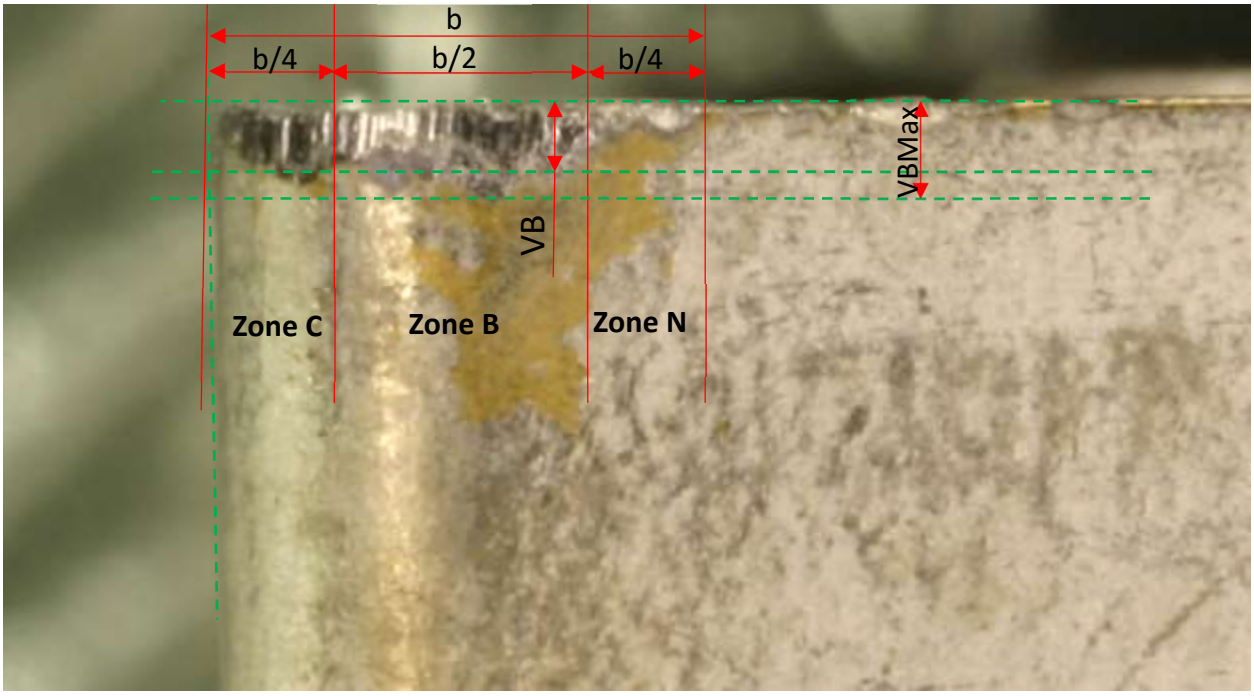


Figure 3-5. Typical flank tool wear with three zones

# CHAPTER 4 ELECTROLESS NICKEL PLATING PROCESS

In this chapter, we briefly summarize the electroless nickel plating onto silicon nitride ceramic which is described in detail in our recently published work. This success in electroless plating approach onto ceramic surface suggests an alternative for a better control of the tool life. That new coating method is then applied on the carbide cutting tool whose the exterior coating layer is ceramic-based material (titanium nitride (TiN) in our study). A characterization of the sacrificial coating will be discussed in this chapter to get more information about the composition of our obtained Ni-B alloy as this parameter is critical with respect to the wear resistance.

## 4.1 Electroless deposition of nickel onto silicon nitride ceramic

The details of the process are described in the journal paper of Zeb, G., Duong, T. L., Balazinski, M., & Le, X. T. (2020). *Direct Electroless Deposition of Nickel onto Silicon Nitride Ceramic: A Novel Approach for Copper Metallization of Micro -/Nano -fabricated Device,* which is in Appendix A.

As anticipated in the introduction, we have developed a new and powerful technique to deposit electrolessly a thin layer of nickel-boron on various kinds of surfaces (conducting and semi-conducting surfaces, oxide, and plastic). Our efficient electroless nickel plating relies on one-step diazonium one-step diazonium-based chemical process without requiring any surface pre-treatment. It is thus interesting to extend the application of that electroless nickel plating to the other materials. We wish next to focus our attention on ceramic surfaces (such as $Si_3N_4$, TiN, TiCN…) which are standout materials particularly for micro-nanofabrication but also for wear resistance applications.

According to the diazonium-based amination described in the section 2, after an immersion for 120 minutes into the diazonium-chemical solution, the amine-terminated groups will be covalently grafted onto silicon nitride (or titanium nitride) ceramic. XPS spectra of the pristine and diazonium-modified silicon nitride surfaces are presented in Figure 4-1. As seen from Figure 4-1 A, the pristine surface shows a typical behaviour of silicon nitride with various peaks : O 1s (at 530 eV), N 1s (at 400 eV), Si 2s (at 152 eV) and 2p (at 102 eV), and a negligible contamination carbon C 1s (at 285 eV) (Zeb et al., 2020). After the diazonium chemical modification, the modified surface is

characterized by an increase in intensity of the C 1s peak which confirms well the presence of the grafted phenyl groups. More importantly, while the typical characteristic of the nitride moiety at 397.7 eV remains unchanged after the diazonium treatment (Figure 4-1B), a new one positioned at 399.5 eV allows us to evidence the presence of the amine-terminated functionalities on the modified surface (Zeb et al., 2020).

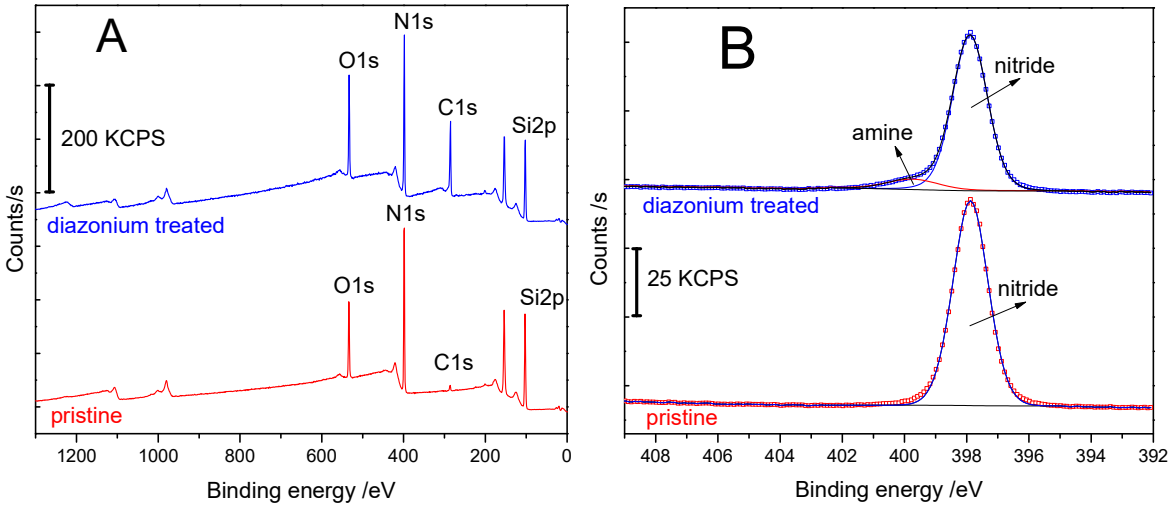


Figure 4-1. XPS survey (A) and high-resolution N 1s (B) spectra of the pristine and diazonium treated surfaces. (Zeb et al., 2020)

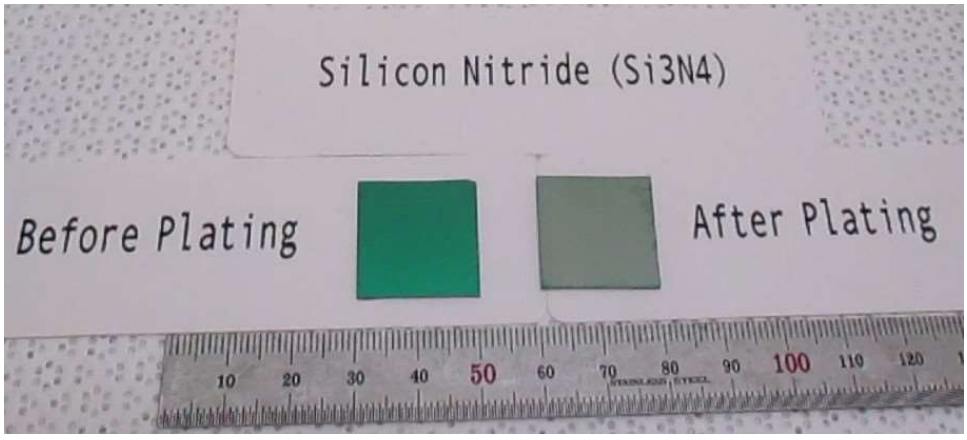


Figure 4-2. Digital photographs of the $Si_3N_4$ surface (left) and nickel film as deposited on $Si_3N_4$ substrate (right) after 6 minutes of processing in the plating bath

An activation of the aminated surface can be easily realized by immersing the modified substrates in a $PdCl_2$/HCl solution for only a few minutes. Under this working condition, the amine groups

are protonated and become positively charged. In contrary, palladium cations exist under the negative chloride complex ($PdCl_4^{2-}$) in 0.5 M HCl solution. They are consequently attracted to the protonated positively charged surface through electrostatic interactions. When we put the activated samples into our plating bath. The reducing agent in the plating solution will reduce first palladium cations ($Pd^{2+}$) to form palladium metal ($Pd^0$) which becomes catalytic nucleus for the subsequent reduction of nickel cations to nickel metal ($Ni^0$). Once nickel metal atoms deposit around palladium noble nuclei, further reduction of nickel cations in the solution are catalyzed by these atomic nickel metals them-self. For this reason, electroless nickel plating is also known as an auto-catalytic deposition. A 3-D nucleation of nickel alloy film grows on the surface as a function of time. The whole activation and plating process can be seen in our appendixed video (see Appendix). It has been observed in our recent work that immersing the silicon nitride substrates for four minutes in the electroless bath is not enough to cover the entire surface. A nickel film entirely covers the silicon nitride substrate after a process duration of 6 minutes as can be visually observed in Figure 4-2. In line with this visual observation, the SEM image recorded on the surface of nickel (Figure 4-3 a) shows a complete coverage of the silicon nitride substrate by an as-deposited nickel film. Besides, it is important to note that the thickness of the nickel film is estimated to be 60 nm (Figure 4-3 b). Once can deduce that the deposition rate is approximatively equal to 10 nm/min.

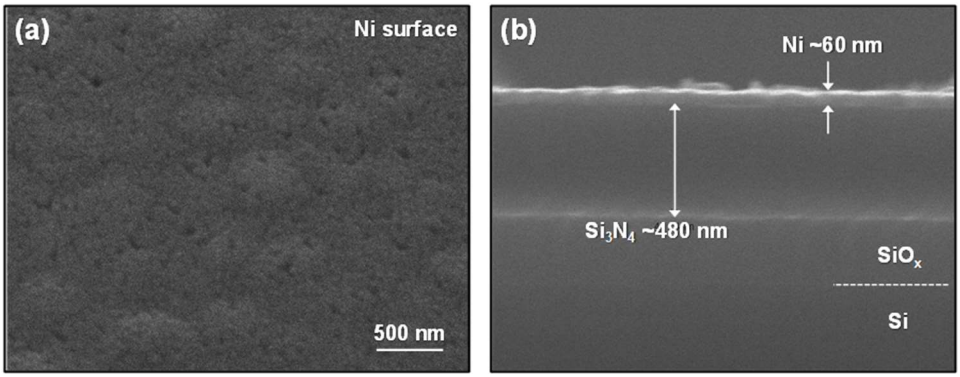


Figure 4-3. SEM image recorded on the surface of nickel showing film coverage (a) and cross-sectional micrograph exhibiting 60 nm of nickel film atop $Si_3N_4/SiO_x/Si$ stack (b). (Zeb et al., 2020)

An electrolessly deposited nickel film is usually a nickel alloy since the reducing agent is involved in the plating process. In our case, because we use dimethylamineborane as reducing agent, boron will co-deposit into the coating film. An estimation of boron percentage is thus necessary as this

parameter directly affects the coating properties (hardness, electric conductivity, resistance to abrasive wear, …). Figure 4-4 presents the EDX spectra of the pristine silicon nitride and the as-deposited nickel film substrate. In addition to the silicon and nitrogen peaks, the pristine surface also contains some negligible amounts of carbon (at 0.277 keV) and oxygen (at 0.525 keV). The observed behaviour is in a good agreement with the XPS discussion given above. The Si/N ratio inside the substrate bulk is evaluated to 0.73 at first approximation. Such the obtained value is close to the stoichiometric ratio of 0.75 ($Si_3N_4$) as expected. The spectrum recorded on the top of nickel surface shows nickel peaks (at 0.742, 0.762 and 0.851 keV) and a boron peak (at 0.183 keV) as well as two small peaks of C and O elements. Si and N elements of the underlying $Si_3N_4$ layer are no longer observed in this spectrum suggesting that EDX is probing only the metallic film. The inevitable native oxide and the atmospheric contamination atop metallization can be considered to explain the presence of C and O peaks (Zeb et al., 2020). From the EDX data, the percentage of boron in weight is estimated at 6.8 % which is comparable to the values published in the literature, from 3 % to 10 % in weight (Zeb, Duong, et al., 2017) & (Vitry & Delaunois, 2015)

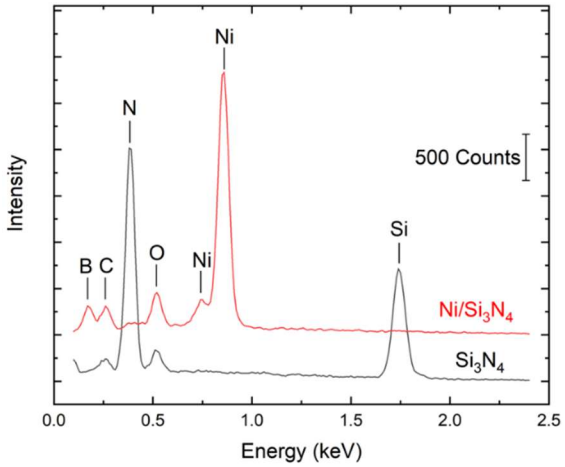


Figure 4-4. EDX spectra of silicon nitride substrate before (black) and after (red) Ni-B deposition (reproduced from (Zeb et al., 2020))

Clearly, the results presented in this section has been proved efficient of our electroless nickel plating through the diazonium-based chemical surface treatment with respect to the ceramic materials. Moreover, our conducted study has allowed us to estimate the percentage of boron within the deposited nickel-boron alloy (Ni-B alloy). The latter parameter is essential for further

applications of the resulting coating film. Fabrication of micro-nanodevices recently reported in Gul et al. (Zeb et al., 2020) can be given here as a representative application. Micro-nanofabrication is however out of the scope of the present thesis which will focus next on characterization of the Ni-B coating onto TiN coated carbide inserts where the surface coverage of the coated Ni-B film and the percentage of boron are essential for the wear resistance applications.

## 4.2 Characterization of the nickel-boron film electrolessly plated onto the cutting inserts.

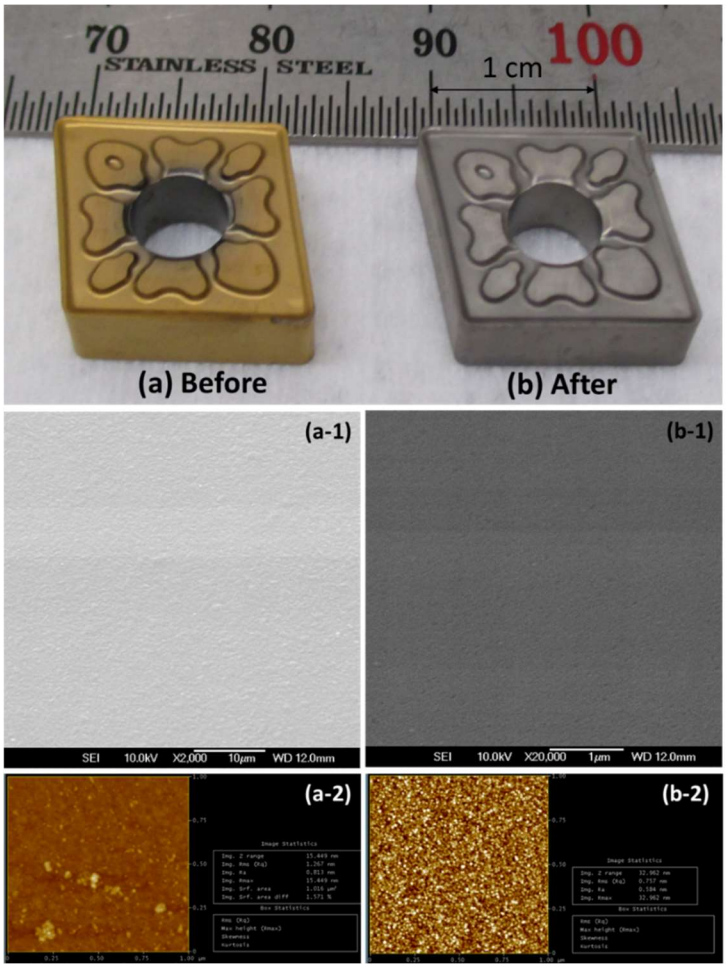


Figure 4-5. (top) digital images of the inserts; SEM and AFM images recorded atop rake face before (a-1,2) and after (b-1,2) electroless nickel plating

The digital photographs of the inserts before and after electroless nickel plating, the SEM and AFM images recorded on the top of the pristine insert surface and the electrolessly plated surface are

presented in Figure 4-5. A nickel film is evidenced from these digital photographs (Figure 4-5 a, b). Another important point to be underlined is that the roughness of the pristine surface looks different compared to that of the plated one (Figure 4-5 a-1 and b-1). The SEM image recorded on plated surface clearly indicates that the plated film is compact and free pinholes at micro scale. It might therefore be required to perform a supplementary analysis at nanoscale. Indeed, the nanoscale AFM images equally point out that the plated surface is fully covered by a homogenous and continuous metallic film (Figure 4-5 a-2, b-2).

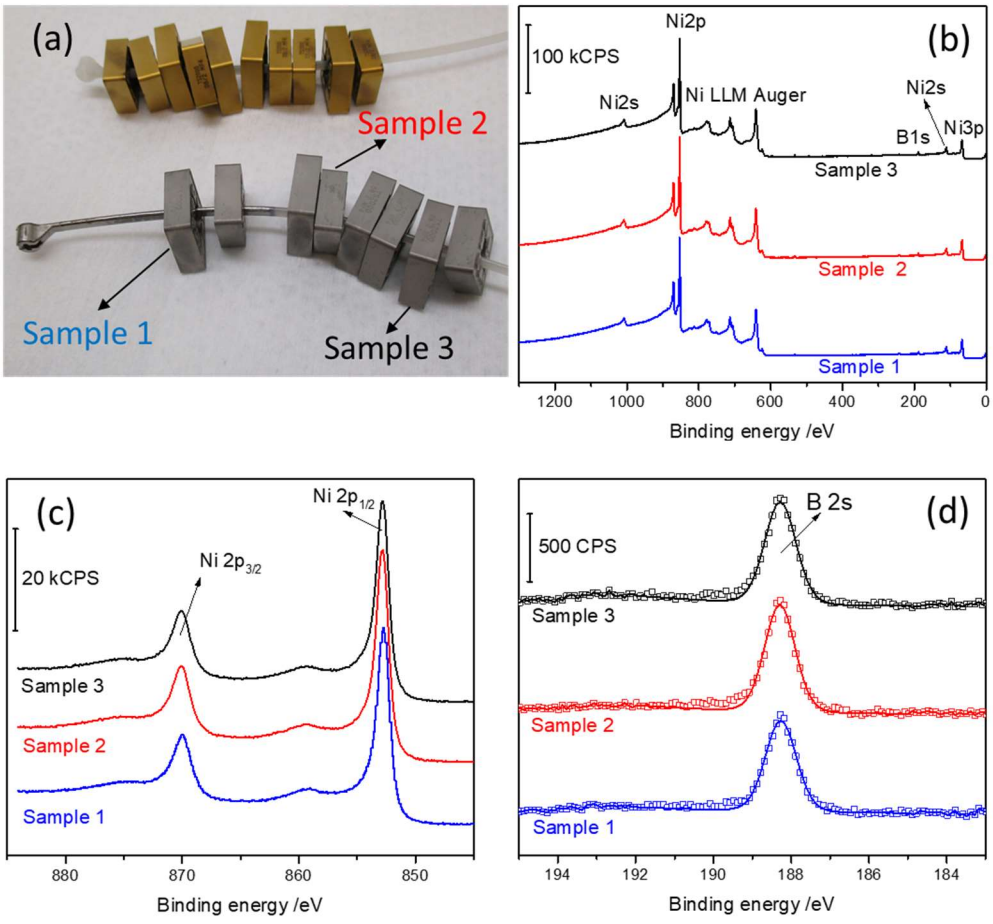


Figure 4-6. (a) digital images of various inserts before and after plating; XPS survey (b), Ni 2p (c) and B 1s (d) of the Ar-ion sputtered nickel surface of three different plated inserts as indicated in image (a)

We have mentioned in the section 4.1 that the percentage of boron is critical due to its effect in various physical properties of the coating film. Especially for wear resistance, the effect of boron

content on hardness of electroless nickel-boron deposits is still an open subject in the literature(Vitry & Delaunois, 2015). These studies have reported that the hardness of nanocrystalline electroless nickel-boron coatings increases with increasing the boron content at least up to 8 weight % boron. In this sense, we have analyzed the composition of our nickel-boron plated film by means of X-ray Photoelectron Spectroscopy. The reason why we chose to work with XPS is that this technique appears as the most efficient in providing the precise information about the percentage of boron within the plated film (Zeb, Duong, et al., 2017).

Here, it is worth reminding that several inserts were plated together under the same condition, it is crucial to get more inside into the producibility from insert to insert. As a result, 3 inserts plated under the same working conditions were taken into account (Figure 4-6a). Figure 4-6 b,c,d presents the XPS survey, Ni 2p and B 1s core level spectra of argon ion sputtered surface of these three inserts. As expected, the survey spectra of these randomly chosen samples are identical, they contain only nickel, boron peaks and a small amount of argon (Figure 4-6 b). This, in other words, means that the plated film is consisted of only nickel and boron. The Ni 2p core level spectra (Figure 4-6 c) show two peaks at 853.1 and 870.5 eV, each with a satellite peak at 859.4 and 874.8 eV, respectively. These peaks are corresponding to Ni $2p_{3/2}$ and $2p_{1/2}$ of nickel under metallic state (Vu et al., 2018). Similar to the Ni 2p spectra, the B 1s core level is best fitted with a unique component at 189 eV (Figure 4-6 d), which ascertains the presence of boride species within the film (Vu et al., 2018).

Detail concerning each element peaks and their corresponding position are listed in the Table 5. The atomic percentages of nickel, boron and argon in the bulk film can be calculated from the XPS data and presented in the table. The weight % of boron within the film can be estimated, at first approximation, through the following relation:

$$wt\ \%\ (B) = \frac{Ar,std(B)}{Ar,std(B)+Ar,std(Ni)*x}$$

with $A_{r,std}$(B) and $A_{r,std}$(Ni) stand for the standard atomic weights of boron and nickel (10.81 and 58.69 respectively).

Three samples appear homogeneous in term of nickel-boron composition. They all contain the same amount of boron, 9.3 ± 0.1 % in weight. Such the homogeneity is interesting from the

industrial point of view. Also, it is important to mention that the chemical composition of the plating batch (pH, nickel and reducing agent concentrations, …) may result in different boron percentages inside the plated Ni-B alloys. This point, nevertheless, needs further investigation in order to confirm the reproducibility of our plating process from bath to bath, and might thus be a subject for a further work in the future. In the following section, we will describe how our nickel-boron alloy plated on TiN coated carbide insert can be beneficial for the wear resistance application.

Table 5. Determination of chemical composition of Ni-B film from XPS data obtained with the Ar-ion sputtered nickel surfaces

| Sample | Element | Position (eV) | Atomic % | Ratio Ni$x$B | wt % (B) |
|---|---|---|---|---|---|
| 1 | Ni 2p | 853.08 | 62.52 | $x$ = 1.82 | 9.2 |
| | Ar 2p | 242.08 | 3.14 | | |
| | B 1s | 189.08 | 34.34 | | |
| 2 | Ni 2p | 853.08 | 62.48 | $x$ = 1.79 | 9.3 |
| | Ar 2p | 242.08 | 2.69 | | |
| | B 1s | 189.08 | 34.83 | | |
| 3 | Ni 2p | 853.08 | 62.40 | $x$ = 1.77 | 9.4 |
| | Ar 2p | 242.08 | 2.34 | | |
| | B 1s | 189.08 | 35.26 | | |

# CHAPTER 5 EFFECT OF SACRIFICIAL COATING ON TOOL WEAR DURING TURNING OF TIMMCS

Tool wear is one of the most important criteria for machinability assessment of the cutting process while tool life has widely been considered to be the primary indicator of the machining cost. This chapter describes the effect of the new sacrificial coating, presented above, on the tool wear and tool life during machining TiMMCs. First, the effect of cutting parameters on the tool wear has been conducted based on the response surface methodology (RSM) according to central composite design (CCD). Here, we use both the original tool and a new sacrificial coating tool. Part of the work then analyzes the tool wear mechanism during the initial wear period that has been reported to significantly affect the tool life. The contribution of such the new nickel coating to the wear mechanism and tool life is discussed.

## 5.1 Effect of cutting conditions on the tool wear during turning of TiMMCs

Table 6 shows the experimental results of flank wear within the initial period when turning TiMMCs, using both original carbide inserts (VBB1) and a Ni/B coated ones for the sacrificial coating (VBB2). The initial wear VBB1 was evaluated in a range of 0.050 – 0.099 mm while VBB2 is 0.046 – 0.081. The improvement of the flank wear when using a sacrificial coating has been found in almost tested conditions. At the center point of the experiment, under cutting speed of V = 45m/min, f = 0.15 mm/rev, and ap 1.5mm the initial wear reduced up to 26.8%. At this point condition, the test is designed repeatedly 6 times as shown in Figure 5-1. We also found that the improvement of the flank wear is negative at some points, even up to 9.7%.

Table 6. Cutting parameters and the flank wear results matrix

| No. | Vc (m/min) | f (mm/rev) | ap (mm) | Original inserts (VBB1) | Ni/B coated inserts (VBB2) | Tool wear improvement after Ni/B coated (%) |
|---|---|---|---|---|---|---|
| 1 | 30.0 | 0.200 | 1.000 | 0.050 | 0.046 | 7.8% |
| 2 | 45.0 | 0.150 | 1.500 | 0.070 | 0.051 | 26.8% |
| 3 | 30.0 | 0.100 | 2.000 | 0.070 | 0.061 | 12.2% |
| 4 | 30.0 | 0.200 | 2.000 | 0.075 | 0.071 | 4.4% |
| 5 | 70.2 | 0.150 | 1.500 | 0.079 | 0.071 | 10.4% |
| 6 | 45.0 | 0.150 | 1.500 | 0.070 | 0.076 | -9.7% |

| | | | | | | |
|---|---|---|---|---|---|---|
| 7 | 45.0 | 0.150 | 1.500 | 0.065 | 0.061 | 5.5% |
| 8 | 30.0 | 0.100 | 1.000 | 0.065 | 0.059 | 8.1% |
| 9 | 45.0 | 0.150 | 1.500 | 0.060 | 0.051 | 14.7% |
| 10 | 60.0 | 0.200 | 1.000 | 0.070 | 0.071 | -2.4% |
| 11 | 45.0 | 0.150 | 1.500 | 0.060 | 0.061 | -2.4% |
| 12 | 19.8 | 0.150 | 1.500 | 0.069 | 0.056 | 18.7% |
| 13 | 45.0 | 0.066 | 1.500 | 0.055 | 0.051 | 6.9% |
| 14 | 45.0 | 0.150 | 2.341 | 0.060 | 0.056 | 6.1% |
| 15 | 45.0 | 0.234 | 1.500 | 0.089 | 0.081 | 9.0% |
| 16 | 45.0 | 0.150 | 1.500 | 0.065 | 0.056 | 13.3% |
| 17 | 60.0 | 0.100 | 1.000 | 0.070 | 0.069 | 0.2% |
| 18 | 60.0 | 0.100 | 2.000 | 0.094 | 0.081 | 13.4% |
| 19 | 45.0 | 0.150 | 0.659 | 0.060 | 0.056 | 6.1% |
| 20 | 60.0 | 0.200 | 2.000 | 0.099 | 0.081 | 18.1% |

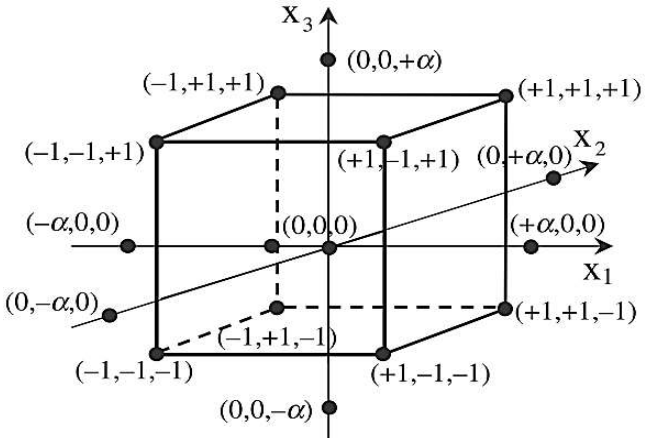


Figure 5-1. Central Composite Design for three factors

In order to describe the empirical relationship between the initial cutting parameters and the response factors of the flank wear on the original inserts ( during the machining process, a general formula is given by Eq. 5.1 (X. T. Duong & Duc, 2013)

$$y = \exp\left[\varphi(V_c, f, a_p)\right] \tag{5.1}$$

Therein, φ is the responsive function of the cutting parameters that depends on the cutting speed, feed rate, and depth of cut. The transformation of the linear regression, see Eq. 5.3 and quadratic regression for three factors, Eq. 5.4 of the cutting parameters are defined through the transformation of the natural logarithm (Choudhury & El-Baradie, 1999; Xuan-Truong & Minh-Duc, 2013).

$$\varphi_q = \beta_0 + \sum_{i=1}^{k} \beta_i x_i + \sum_{i=1}^{k} \sum_{j=i+1}^{k} \beta_{ii} x_i x_j + \sum_{i=1}^{k} \beta_{ii} x_i^{\,2} \qquad (5.2)$$

where $\delta_0$ *and* $\beta_0$ are the free terms of the regression equation; $\delta_1, \delta_2, \delta_3$ and $\beta_1, \beta_2 \ldots \beta_k$ are the linear terms while the $\beta_{11}, \beta_{22} \ldots \beta_{kk}$ and $\beta_{12}, \beta_{13} \ldots$ are quadratic and the interaction term. All these parameters are experimentally determined.

These results, in turn, are served to calculate the statistical analysis of variables (ANOVA) for the cutting parameters to find the cutting condition which significantly affects the response factors. Therefore, the statistical features such as R-Squared, R-adjusted squared, P-value and F-ratio were also applied to analyze the results. Variance analysis of ANOVA for Response Surface Quadratic model for the tool wear is shown in Table 7 and Table 8.

Table 7. ANOVA for Response Surface Quadratic model Vbb1 for original inserts

| | **Sum of** | | **Mean** | **F** | **p-value** | |
|---|---|---|---|---|---|---|
| **Source** | **Squares** | **df** | **Square** | **Value** | **Prob > F** | |
| Model | 0.31 | 9 | 0.035 | 1.25 | 0.3648 | not significant |
| *A-Cutting Speed Vc* | *0.15* | *1* | *0.15* | *5.37* | *0.043* | |
| *B-Feed rate f* | *0.037* | *1* | *0.037* | *1.34* | *0.2747* | |
| *C-Depth of cut ap* | *0.043* | *1* | *0.043* | *1.54* | *0.2432* | |
| *AB* | *2.15E-03* | *1* | *2.15E-03* | *0.078* | *0.7863* | |
| *AC* | *3.93E-03* | *1* | *3.93E-03* | *0.14* | *0.7145* | |
| *BC* | *0.019* | *1* | *0.019* | *0.68* | *0.4291* | |
| $A^2$ | *0.027* | *1* | *0.027* | *0.97* | *0.347* | |
| $B^2$ | *0.036* | *1* | *0.036* | *1.3* | *0.2805* | |
| $C^2$ | *5.83E-06* | *1* | *5.83E-06* | *2.10E-04* | *0.9887* | |
| Residual | 0.28 | 10 | 0.028 | | | |
| *Lack of Fit* | *0.16* | *5* | *0.032* | *1.41* | *0.3588* | *not significant* |
| *Pure Error* | *0.12* | *5* | *0.023* | | | |
| Cor Total | 0.59 | 19 | | | | |

Table 8. ANOVA for Response Surface Quadratic model Vbb2 for sacrificial coating inserts

| | **Sum of** | | **Mean** | **F** | **p-value** | |
|---|---|---|---|---|---|---|
| **Source** | **Squares** | **df** | **Square** | **Value** | **Prob > F** | |
| Model | 0.36 | 9 | 0.04 | 1.76 | 0.1959 | not significant |
| *A-Cutting Speed Vc* | *0.11* | *1* | *0.11* | *5* | *0.0492* | |
| *B-Feed rate f* | *0.035* | *1* | *0.035* | *1.55* | *0.2416* | |
| *C-Depth of cut ap* | *0.095* | *1* | *0.095* | *4.21* | *0.0674* | |
| *AB* | *7.75E-03* | *1* | *7.75E-03* | *0.34* | *0.5706* | |
| *AC* | *3.97E-03* | *1* | *3.97E-03* | *0.18* | *0.6835* | |
| *BC* | *0.019* | *1* | *0.019* | *0.83* | *0.3835* | |
| $A^2$ | *0.057* | *1* | *0.057* | *2.51* | *0.1443* | |
| $B^2$ | *0.026* | *1* | *0.026* | *1.16* | *0.3068* | |
| $C^2$ | *2.71E-03* | *1* | *2.71E-03* | *0.12* | *0.7357* | |
| Residual | 0.23 | 10 | 0.023 | | | |
| *Lack of Fit* | *0.2* | *5* | *0.04* | *8.47* | *0.0175* | *significant* |
| *Pure Error* | *0.024* | *5* | *4.76E-03* | | | |
| Cor Total | 0.58 | 19 | | | | |

The model F-value of 1.25 and 1.76 implies the models Table 7 and Table 8 are not significant relative to the noise. There is a 36.48 % chance in the first model that an F-value this large could occur due to noise, while only a 19.59 % chance in the model with sacrificial coating could occur due to noise. In addition, "A negative " "Pred R-Squared" of the Table 8 implies that the overall mean maybe a better prediction for the tool wear than the original model. As a result, the ratio of 5.624 indicates an adequate signal. Indeed, this model can be used to predict the tool life.

According to the experimental results, we obtained the set of control points for the quadratic and interaction term. Tool wear during machining of TiMMCs of the model (5.2) is thus expressed as follows:

$$VBB_1 = e^{\wedge}(-2.84+0.1*V+0.052*f+0.056*ap+0.016*V*f+0.022*V*ap+0.048*f*ap+0.05*V^2+0.05*f^2+e.36E-004*ap^2) \quad (5.3)$$

$$VBB_2 = e^{\wedge}(-2.74+0.091*V+0.051*f+0.083*ap+0.031*V*f+0.022*V*ap+0.048*f*ap+0.63*V^2+0.43*f^2-0.014*ap^2) \quad (5.4)$$

These equations permit us to determine the tool wear behavior at various cutting conditions. More importantly, the effect of the sacrifice coating layer on the tool wear is more recognizable for analysis in the coming section. The relationship between the flank wear of the original tool with Ni/B coated cutting tool and cutting conditions is therefore produced procedurally into the 3D model as illustrated in Figure 5-2 to Figure 5-4.

It is observed that the cutting speed and feed rate effect significantly the tool wear on both original and Ni/B coated inserts, while the depth of cut plays a minor role on the flank wear. The improvement of tool wear has been found under medium and low feed rate for all cutting speed and depth of cut. At the medium value of the feed rate, the tool wears reduced at all speed conditions, Figure 5-2 (b).

(a) Flank wear on the original inserts

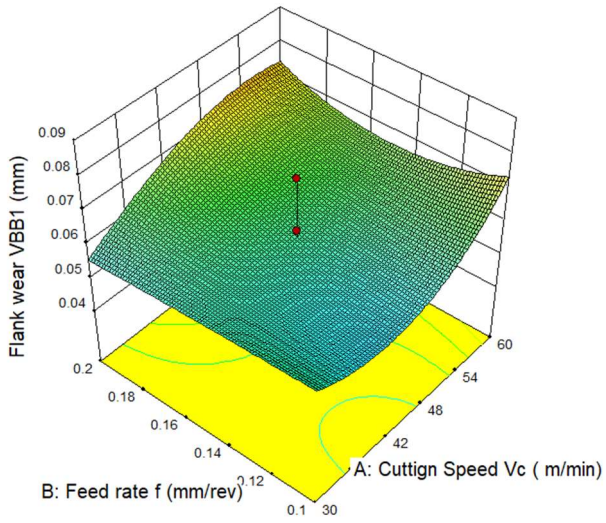


(b) Flank wear on the sacrifice inserts

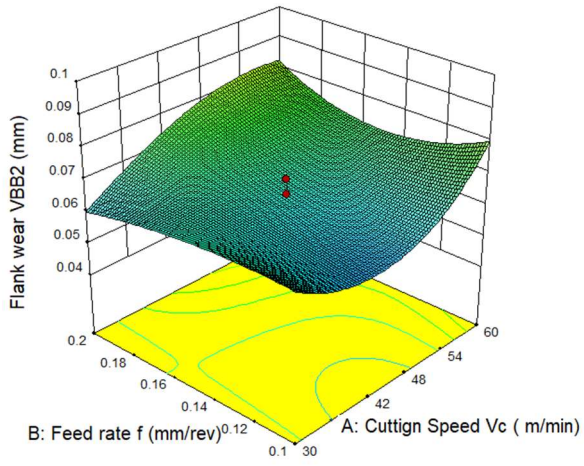


Figure 5-2. Effect of cutting speed and feed rate on the flank wear

(a) Flank wear on the original inserts (b) Flank wear on the sacrifice inserts

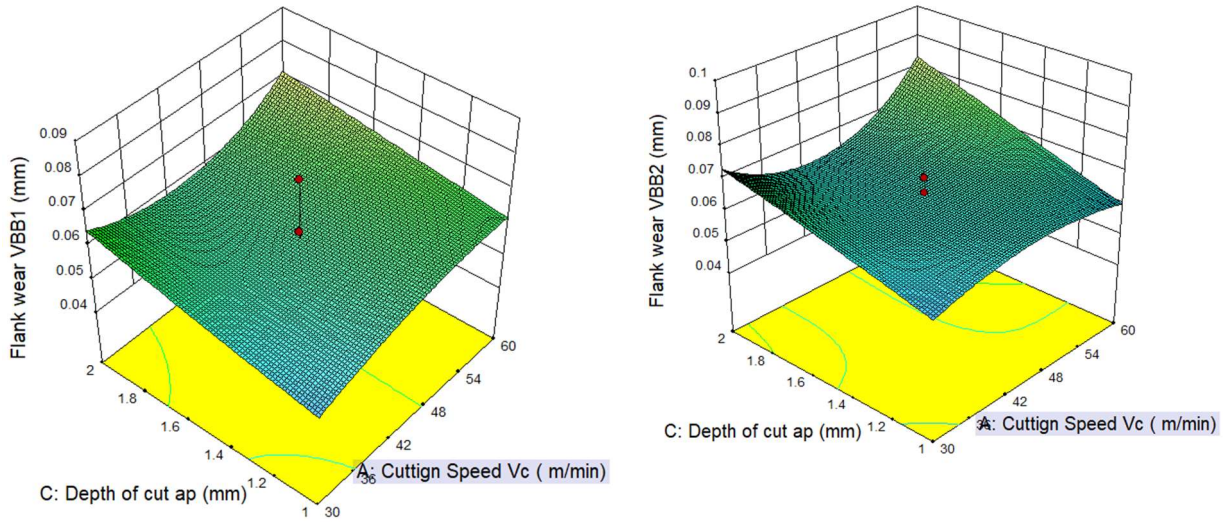


Figure 5-3. Effect of cutting speed and depth of cut on the flank wear

(a) Flank wear on the original inserts (b) Flank wear on the sacrifice inserts

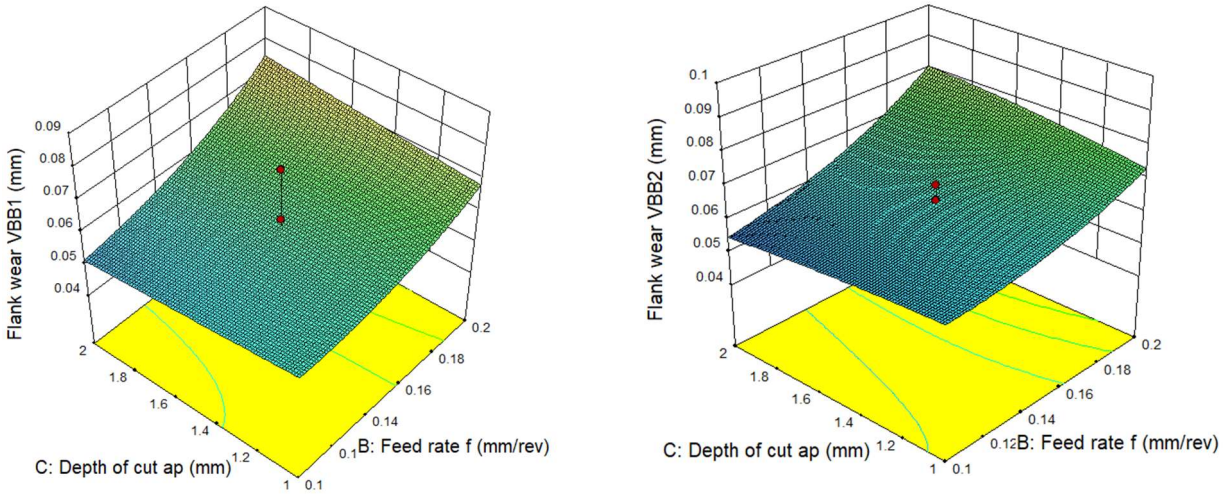


Figure 5-4. Effect of feed rate and depth of cut on the flank wear

This phenomenon is explained through the contribution of the sacrificial coating Ni/B to the wear mechanism (around 3 to 5 %). To validate the influence of the new coating layer under the mentioned conditions, the effect of cutting parameters on the cutting force has been investigated,

as given in Figure 5-5 (a,b and c). As seen here, with a feed rate less than 0.15 mm/rev the cutting force has not changed much under all the tested cutting conditions. At the higher feed rate and the depth of cut, the cutting force increase significantly, Figure 5-5 (c).

When the cutting speed and feed rate increase considerably, the abrasion wear is the dominant mechanism. At the low cutting speed and feed rate, the main wear mechanism is adhesion. Indeed, when a new material layer was coated onto the tool, the edge radius of tool will be increased, at low cutting speed and feed rate, the tool is not really cutting the materials but pushing. This leads to a high cutting force and high temperature which are the main reason for resulting adhesion wear. At low speed and low feed, a high BUE formation and ploughing result in chipping at the tool edges. We also observed that at high depth of cut, the force is very high, and it pushes the tool on the workpiece and therefore the hard particles of workpiece will abrade the tool.

In addition, the increase in cutting forces leads to high contact stress and high friction between the tool-workpiece with the Ni/B coating layer interface. Accordingly, several hard particles including the sacrificial coating get into contact and are involved in the thermal and chemical processes. The effect of this layer on the wear mechanism will be discussed in the next section.

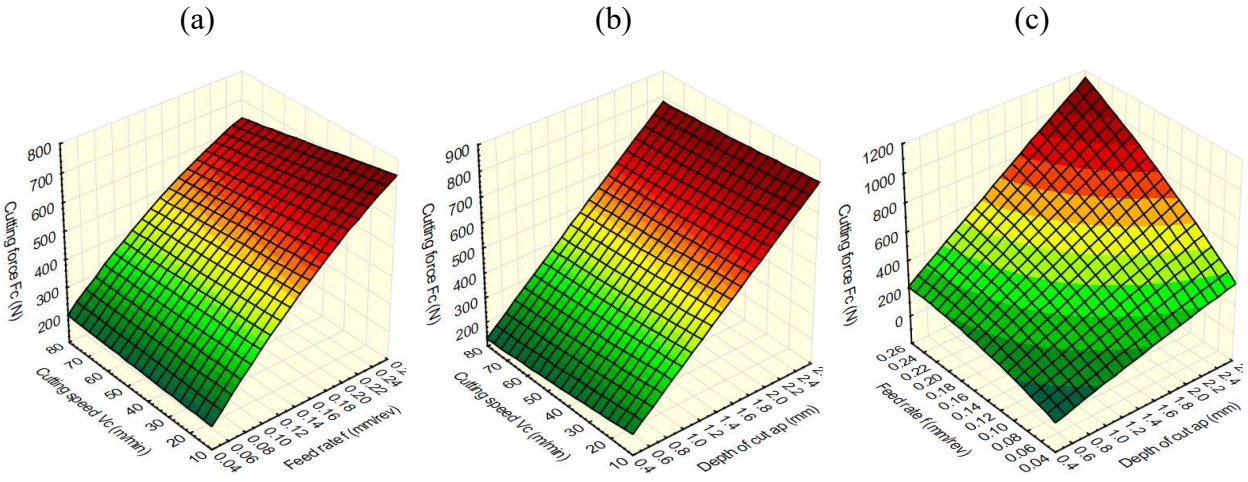


Figure 5-5. Effect of cutting parameter on the cutting force

## 5.2 Effect of the sacrificial coating Ni/B on the wear mechanism during turning of TiMMCs.

Since the TiMMCs is very hard to machine material due to the combination of both machining problems associated with titanium alloys and metal matrix composites (MMCs). The most difficult characteristics of titanium alloys are high reactivity, low thermal conductivity, and maintaining their high strength and hardness at elevated temperatures (X. Duong et al., 2016; Escaich et al., 2020). The adhesive, build-up edge, and diffusion play a key role in the wear mechanism (Vereschaka et al., 2019). On the contrary, the difficult characteristic of MMCs is the abrasive properties of hard particle reinforcement in the TiMMCs. The MMCs reinforced with ceramic particulates, especially with the TiC provide better strengths and higher wear resistance at elevated temperatures (Campbell, 2006). Therefore, the abrasion wear is the most important mechanism during machining of MMCs that resulted in fast tool wear (Salur, Aslan, Kuntoglu, Gunes, & Sahin, 2019).

In order to analyze the effect of the hard particles on the wear mechanism, characterization of Ti-MMCs with EDS has conducted as shown in Figure 5-6. An unpolished sample of Ti-MMCs whose the chemical compositions are given in Table 2 was cleaned under the condition of 20 minutes immersion in ultrasonic for each cleaner: acetone, isopropyl alcohol, and methanol. Base on the SEM micrographs of the Ti-MMCs sample in Figure 5-6 (a) and (b). The dimension of the TiC particle was measured to 2.3 μm. This is in a good agreement with a previously published study (X. Duong et al., 2016). Therein, the observed dimension of TiC is smaller than 25μm.

Figure 5-6 (c and d) show that the dominant elements in the chemical composition of the selected surface area: 88.5% titanium (Ti) as expected, found to be rich, 5.6% aluminum (Al), 3.7% vanadium (V), that are the constituent components of Ti-6Al-4V matrix and 2.2% carbon (C) belongs to TiC particles as reinforcement in Ti-MMC (Kamali Zadeh, 2016). In the case study, the increase in thrust leads to high contact stress and high friction between the coating and workpiece surfaces at the tool-workpiece interface.

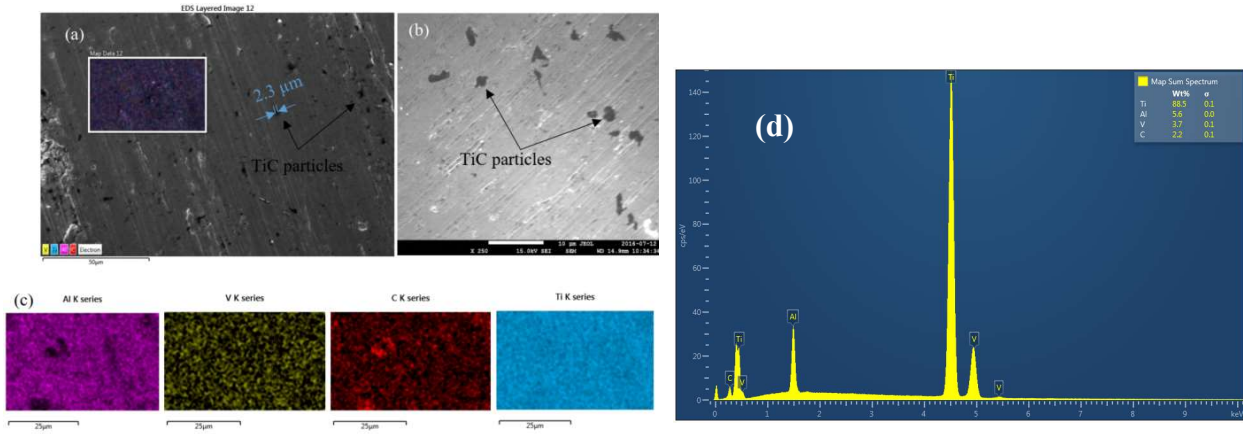


Figure 5-6. The SEM micrographs of the Ti-MMCs sample

(a) SEM micrograph of an unpolished Ti-MMC sample the TiC particles dispersed into the material is specified, (b) higher magnification of the surface and TiC particles; (c) mapping of the different chemical composition of Ti-MMC sample; (d) EDS analysis on the surface of the sample (Kamali Zadeh, 2016)

Consequently, several hard particles in the damaged zones are taken out follows by the chip formation with a high wear rate due to overload of mechanical tensile stresses, as illustrated in Figure 5-7. The abrasive TiC particles on the chip will abrade the cutting tool significantly, resulting in high abrasion wear.

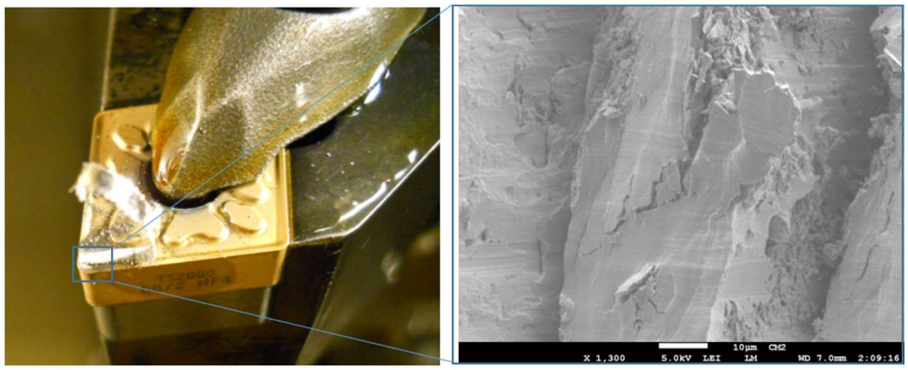

Figure 5-7. Chip formation during turning of TiMMCs

According to the increase of cutting force and temperature at the first moment of cutting; at the tool and machined surface interface, the cutting tool material tends to react chemically with titanium and causes adhesion of the workpiece material to the cutting edge as shown in Figure 5-8

(a). Thanks to the thin coated layer of nickel-boron on this cutting tool, the elements react spontaneously with atmospheric oxygen while the titanium and aluminum are oxidized at the high pressure and elevated temperature under the cutting conditions.

Figure 5-8 (a, b and c) present the contribution of the Ni-B coated carbide inserts under the condition of Vc=30 m/min, f=0.2 mm/rev, ap= 1 mm at the cutting time of 6.5 second. Under the same cutting condition, Duong et al, (X. Duong et al., 2016) reported that the effect of the hard particle of titanium carbide reinforcement lead to the cutting edge being directly weakened by oxidation of the workpiece material and being easily taken away by the chip with high wear rate. However, the coated nickel-boron film layer on this insert estimated only 100 nm has involved the machining process that still be found to be rich, Figure 5-8 (b). The chemical composition of this film is critical due to its effect in various physico-chemical properties of the coating layer.

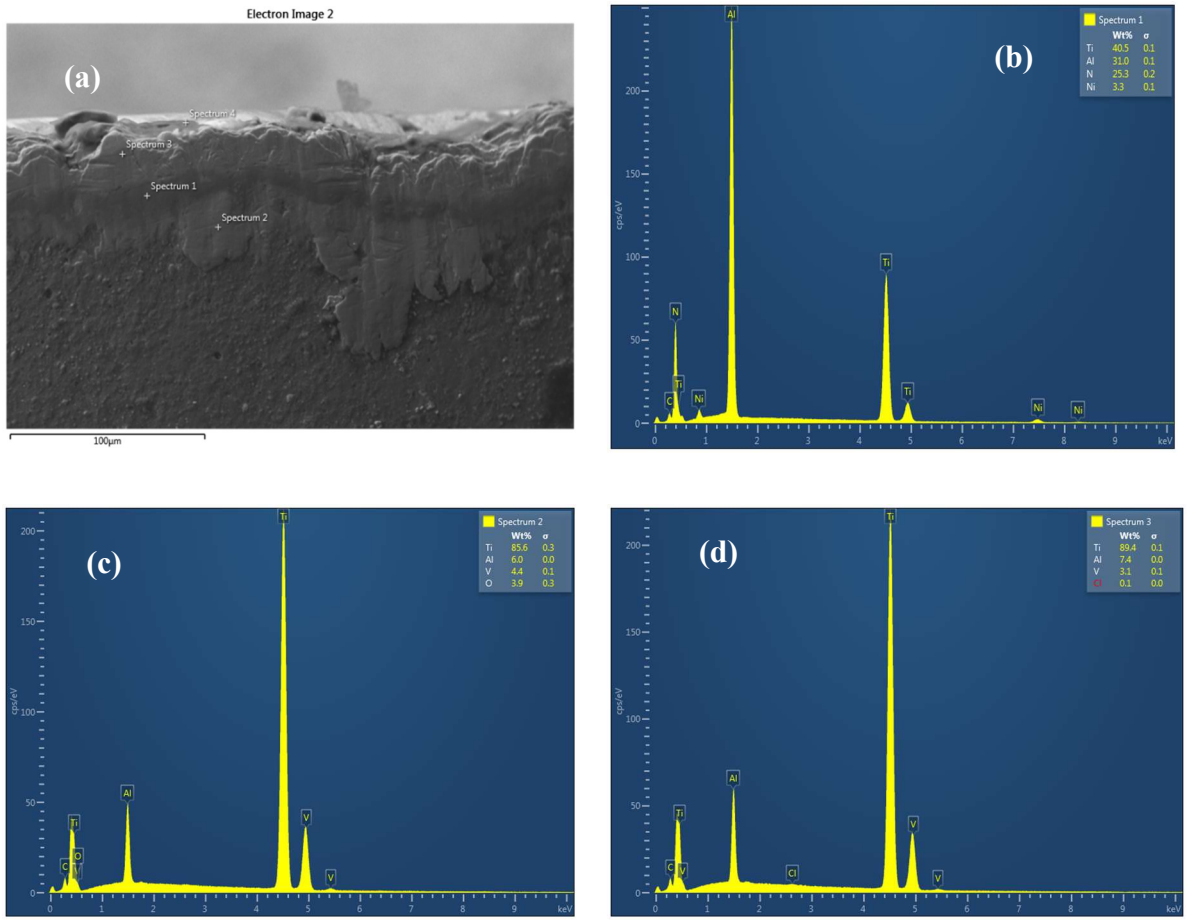


Figure 5-8. Flank wear and EDS spectrums and corresponded deposition layers

SEM and AFM analysis have been carried out (Figure 5-9 ) in order to validate the contribution of the electroless nickel-boron plating on the tool wear mechanism. The figure shows the dominant wear mechanisms. High amount of Ti and Al shows high adhesion. The nickel coating seems to be covered completely by the adhered material. However, the percentage of nickel is still found up to 3.3% as shown in Figure 5-8 (b). In fact, the subtraction of this insert (or the original one) has been coated by PVD method with the (Ti,Al)N+TiN. In this case, the low thermal conductivity of titanium alloys under high tress pressure leading the gradient temperature at the tool-workpiece-chip interfaces. Residual stresses specially at the tool tip, can affect the homogeneity of the coating and its coverage.

Hence the surface of workpiece material and coating tool layer get into contact and resulting in residual stress in the feed direction (Zhao & Liu, 2020). As a result, a micro-welding and built-up-edge (BUE) are formed under sufficient pressure at the cutting edge under all experimental cutting conditions (X. Duong et al., 2016; Memarianpour, Niknam, Turenne, & Balazinski, 2018).

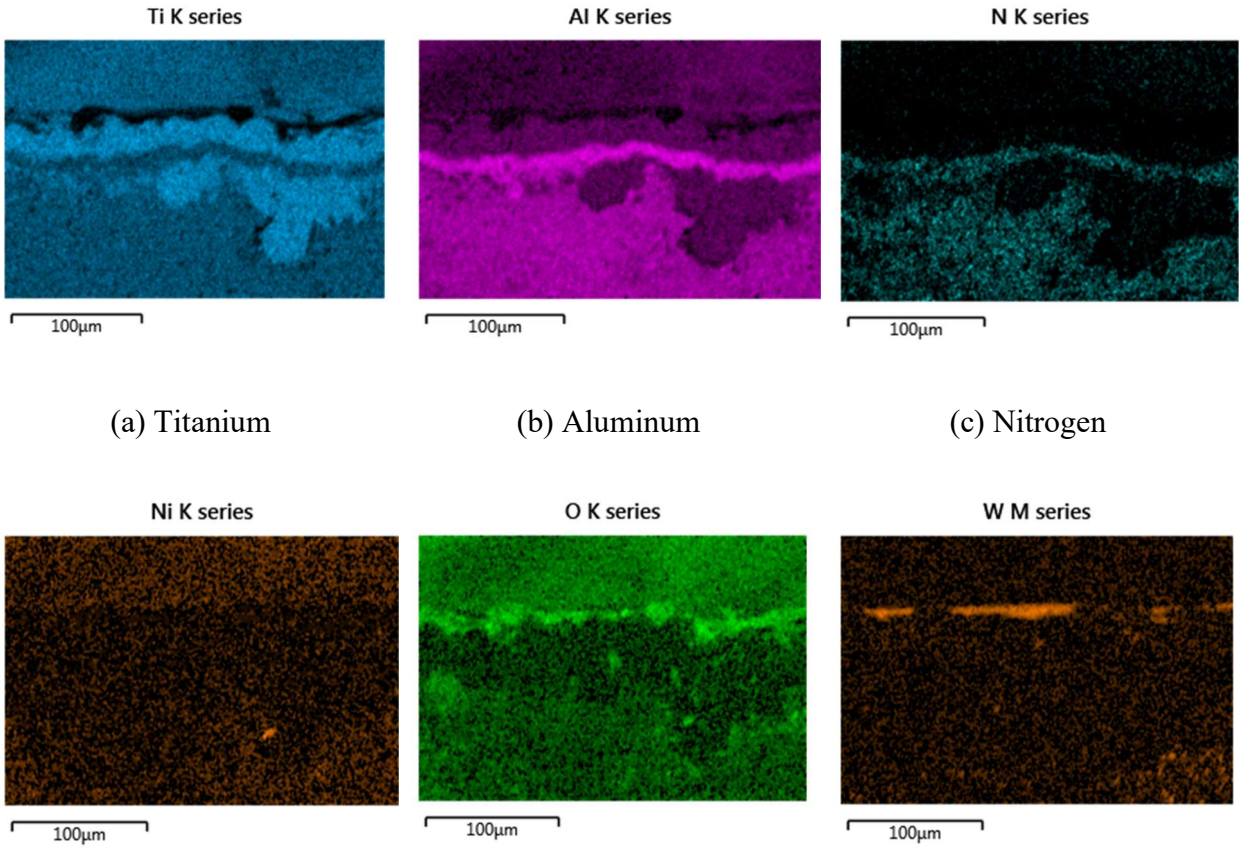


(a) Titanium (b) Aluminum (c) Nitrogen

(d) Nickel (e) Oxygen (f) Wolfram

Figure 5-9. Elemental maps of the entire zone in the cutting tool

The sacrificial coating that we used within this project contains roughly 100 nm; therefore, it may be removed rapidly from the beginning of the machining process. However, the initial wear period has taken place during a very short periods of time therefore the effect of this sacrificed coating layer on to the tool wear mechanism will be investigated in the initial wear period. In addition, the abrasive particles that adhered to the cutting tool as a whole to involve the cutting process; the physical properties of the tool material are changed and also affect the tool performance.

In the decomposed structure, the diffusion of elements is enhanced from the TiMMCs and the substrate tool materials (Calamba et al., 2019). Consequently, the tool layer damage, friction, and adhesive wear occur simultaneously at the flank face; they react chemically with each other at elevated temperature and forming a smooth layer has been reported as a “wear shield” layer at the

first transaction period (X. Duong et al., 2016; Kamali Zadeh, 2016). More importantly, the initial wear mechanism has been reported to be sensitively affected tool wear evolution in time and tool life.

The present of chemical compositions under difference cutting speed of 60, 40 and 20 m/min are expressed in Figure 5-10 (a), (b) and (c) respectively.

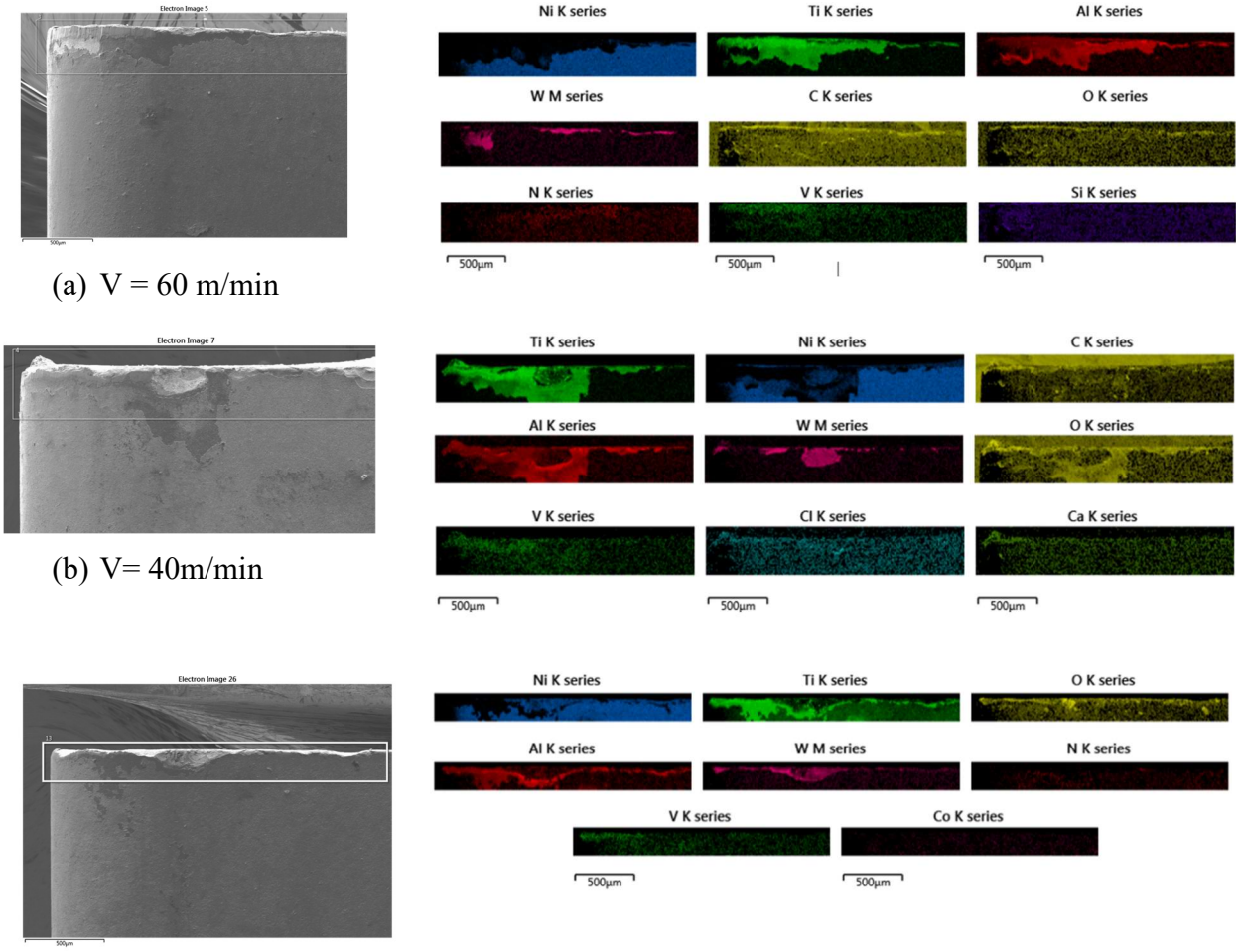


(a) V = 60 m/min

(b) V= 40m/min

(c) V= 20m/min

Figure 5-10. EDS mapping analysis of SEM micrograph

After 0.5 second of cutting the key elements are exhibited in the EDS mapping, their distribution and locations on the flank face of the cutting tool. Indeed, the titanium and aluminium exist on both workpiece and coating layer tool materials, but Vanadium (V) appears only in the workpiece composition (Table 2) which relates to the adhesion mechanism (Seyed Ali Niknam, Saeid

Kamalizadeh, et al., 2018). The presence of Ni in the wear region and its contribution will be further discussed in this section.

In addition, the coating layers of the original inserts were fundamentally found on the cutting edge where the presence of Ti, Al elements were found to be rich in the wear surface under all the tested cutting speeds. They are transferred from the coating layer with aluminum and titanium in the workpiece material. It is advised that N K series elements belong to machined tool Ti-MMCs matrix (Ti-6Al-4V) due to the low concentration of nitrogen. The observed N on the flank face was deposited from the workpiece material. We also observe certain amounts of vanadium (V) in V K series on the wear surface. It is believed that the existence of vanadium (V) came from the matrix Ti-6Al-4V of workpiece material.

Tungsten (W) and cobalt (Co) are the substrate of tool. They are considered as core and binder one, as can be found in the Table 2. We obtained here (W) in W M series mostly in the region near the cutting edge. Additionally, the color of W M series changes along with the width od worn-out edge under all the tested conditions. This means that the coating was removed, and the substrate of the cutting tool was explored. Considering the Ni map of a higher cutting speed in Figure 5-10 (a), this image clearly shows that the coating is delaminated. In the cross-section images, only a rather small content of Ni is observed, while W content is very high. Actually, both the coatings (Ti-Ni and Ni-B) are delaminated. In Figure 5-10 (b, c), the delamination is still found at low speeds, but it is not continuous, since the adhesion and built-up edge are more severe at low speeds. BUE has a cyclic nature, forms and deforms, when deforms can take a piece of tool and coating as well and result in chipping. Both phenomena are observed here. However, in this case, the coated elements of titanium, aluminum and nickel are primary found in the flank wear face at low speed (Figure 5-12 (b) and Figure 5-13 (b)). These elements are less significantly in the higher cutting speed as shown in Figure 5-13 (b).

The presence of 0.2% Ni on the wear surface under cutting speed of 40 m/min, Figure 5-12; the BUE has still generated by plastic deformation under high pressure and thermal softening at high temperature within only 0.5 second of cutting.

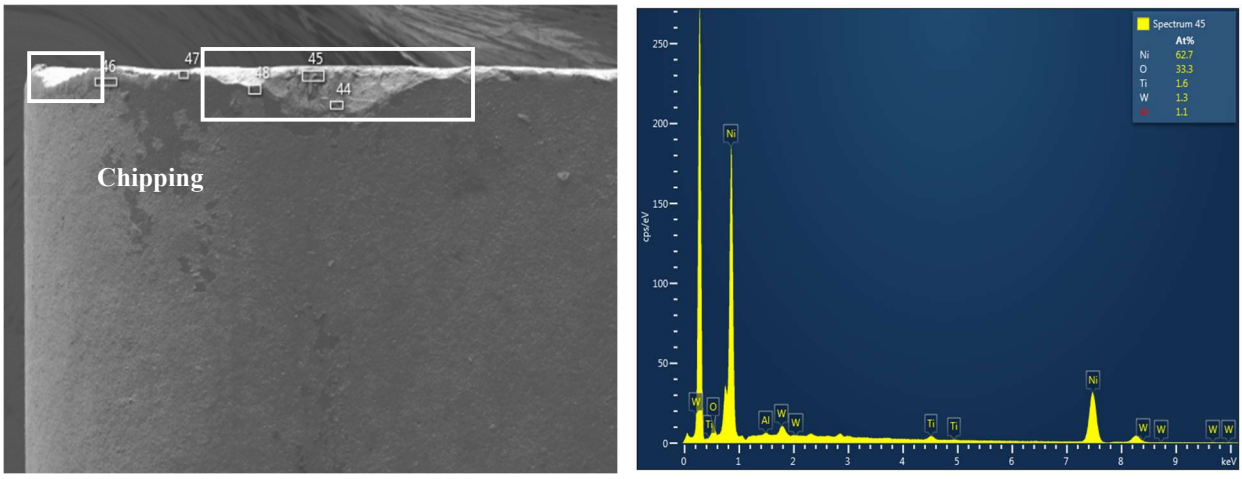


(a) (b)

Figure 5-11. Vc= 20m/min (a) A SEM image shows EDS analysis location and wear mechanism (b) EDS spectrum of the insert with cutting time 0.5 seconds

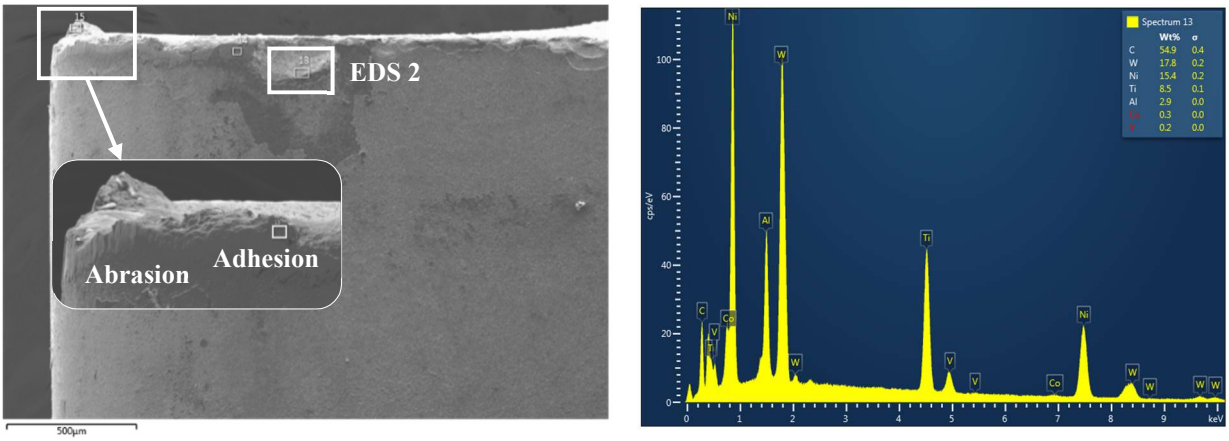


(a) (b)

Figure 5-12. Vc= 40m/min (a) A SEM image shows EDS analysis location and wear mechanism (b) EDS spectrum of the insert with cutting time 0.5 seconds

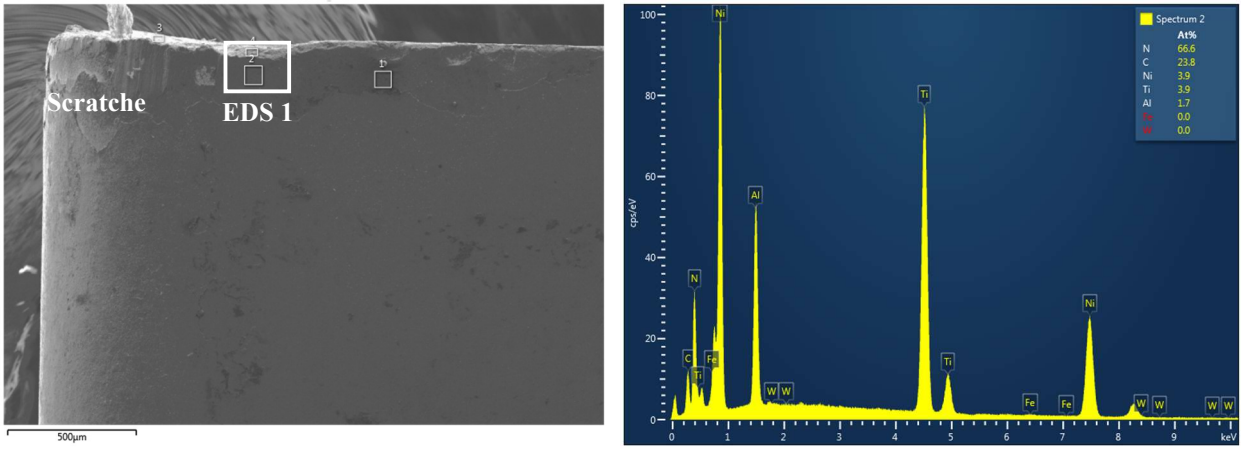


(a) (b)

Figure 5-13. Vc= 60m/min (a) A SEM image shows EDS analysis location and wear mechanism (b) EDS spectrum of the insert with cutting time 0.5 seconds

The EDS results show that the elements such as: nickel (Ni), oxygen (O), and nitrogen (N) which typically exist in tool surface and titanium (Ti), carbon (C) and aluminum (Al), frequently exist in both the workpiece and tool material. Tungsten (W), cobalt (Co) belongs to carbide substrate. At the first moment of cutting, the tool wear is mainly found in the flank face with various wear mechanisms. It is observed that the cutting edge deformed (chipping and BUE) at the lower levels of cutting speed. The scratches (Vc=60m/min), abraded edge, (Vc=40 m/min) and chipping (Vc=20-40 m/min) were found emerging at the flank face of the tool. It is explained as follow: when the coating is applied, it can increase the cutting-edge radius. Thus, at low cutting speed and feed rates, ploughing can occur and result in severe tool chipping. In addition, at the higher cutting speed, under the high force, the hard particles of workpiece might be disintegrated and scratched on the surface of tool.

Furthermore, the deformation of cutting edge increases the cutting forces and cutting temperature. Particularly, thrust force causes the high friction between tool-workpiece interface, and high contact stress, while the overloaded tensile stress also takes out the hard particles in the deformed zone and leads to a high wear rate. The tool layer elements then react instinctively with atmospheric oxygen. Titanium and aluminum are oxidized especially at elevated temperatures and high pressure of the cutting conditions. Therefore, TiC particles cause high abrasion wear, specially at higher

speeds. Debonding of TiC particles from the workpiece material caused 2-body and 3-body abrasion wear mechanisms.

Based on the EDS spectra at the chosen points, the chemical composition of the elements of titanium, aluminum, vanadium, carbide, and nickel are principally found in the abrasive and adhesive surface and BUE as well. The cutting tool materials chemically reacted with titanium. This chemical reaction affects the wear mechanism at the initial cutting stage. However, the adhesion wear is not frequently observed on that face under various conditions. This wear behaviour is clearly affected by the coating sacrificed material. At higher cutting speed, scratches appear from the nose and gradually increase to the flank face, as shown in Figure 5-13Figure 5-13 (a). In stead of the adhesion and diffusion wear that has been reported in various recently published works, we have found in this work that the abrasive wear is the most important mechanism; where, the Ni presence to 3.9%, Figure 5-13 (b). Also, the chipping at lower cutting speed was found due to applying of sacrificial coating, and the delamination happened at most of the cutting conditions. Clearly, the presence of our thin film sacrificial coating on the cutting tool has changed the chemical wear behaviour and the wear mechanism at the first wear period. Thus, the effect of this layer on the tool life is further discussed in the next coming section.

## 5.3 Effect of the sacrifice coating layer on the tool life when turning TiMMCs.

As already anticipated in the previous section, TiMMCs is a very difficult to machine material due to high strength, high stiffness, and wear resistance at high temperatures; the tool life when machining this material using a PVD coated carbide or even for most of the available coating tools is thus very short. Turning under cutting speed of V = 60m/min, feed rate f = 0.15 rev/min and depth of cut ap = 1.5 mm the tool life recorded less than sixty seconds. Supporting this machining characteristic, Kamali Zadeh confirmed in (Kamali Zadeh, 2016) that the transition point occurs less than one second of the machining of this material. It is reported that the initial wear behavior plays a significant role on the tool life when machining TiMMCs. In order to extend the tool life, Duong, X.T et al. (X. Duong et al., 2016) proposed a chaotic model as shown in Figure 5-14. On the basis of this model, the authors proved that controlling the initial conditions can improve tool life up to 24.5% when machining the TiMMCs. This theory has been explained by sensitive depend on the initial conditions of the tool life.

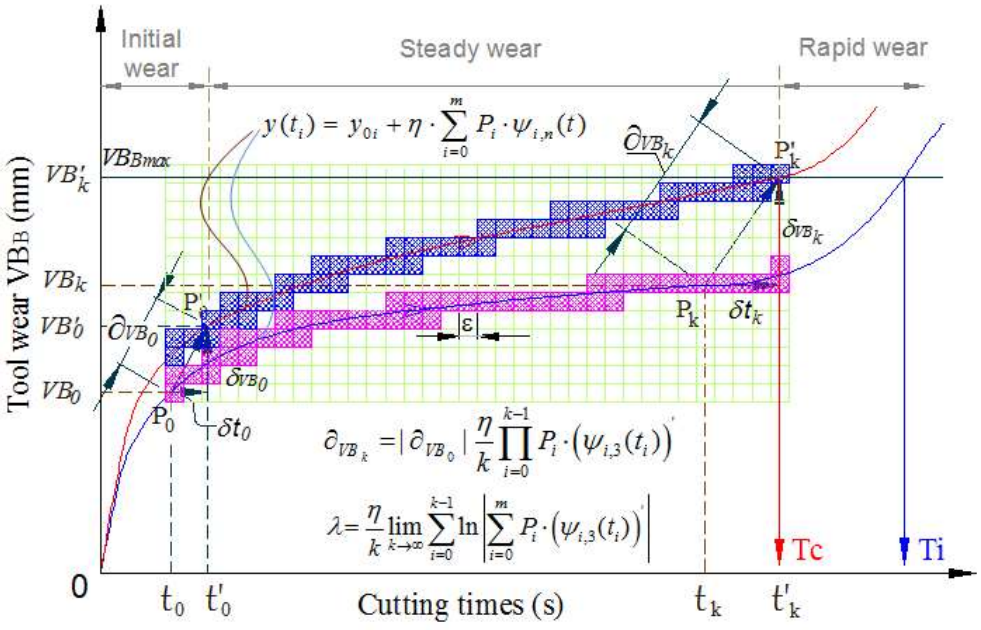


Figure 5-14. Chaos theory characterized tool wear during the machining process

(reproduced of (X. T. Duong, 2015a))

In line with this model, we proposed herein a novel method to change the initial wear mechanism by electroless plating of a sacrifice thin film layer onto the cutting tool. The promising results discussed in chapter 4 and chapter 5 allow us to continuously investigate the effect of the sacrificial coating of Ni/B on tool life during the machining of TiMMCs.

To analyze the effect of Ni/B thin film layer on the tool life during turning process numerous turning tests were performed under dry condition. Our obtained results from the phase 1 of the experiment (section 5.1) evidence that the cutting speed significantly impacts tool wear. In the phase 2, our experimental test is thus performed with different cutting speed Vc = 20, 40, 60 rev/min while depth of cut and feed rate are kept constant ap = 1 mm and fr = 0.15 mm/rev respectively. Each experiment condition was repeated three times for both sacrifice coating layer and original inserts. The average results are then generated the tool wear evolution over time. Figure 5-15 shows the flank wear evolution under a cutting speed of V= 20 - 60 m/min using a PVD coated carbide insert and the nickel-boron coated inserts (PVD coated based).

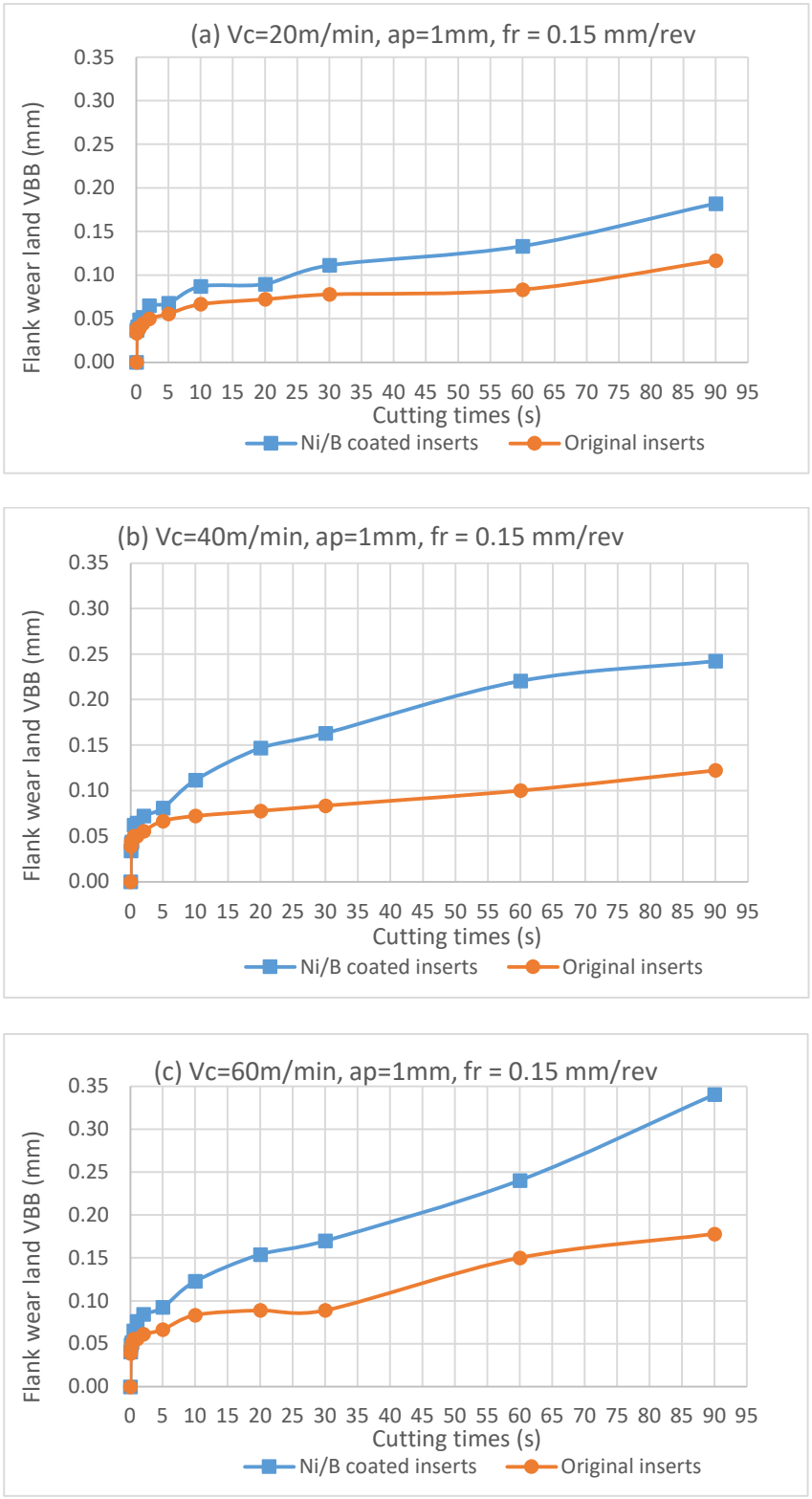


Figure 5-15. Tool wear evolution using original inserts and sacrificial coating inserts

As observed from Figure 5-15, the initial wear increases very fast within a few seconds of cutting for both cases of cutting tool; however, the initial wear values are taken much more than the steady wear period. The effect of chemical stresses at the increased cutting temperature during accelerated cutting force leads to layer damage, friction - tribological wear, and adhesion. It can be given here for the explanation. In fact, the adhesion with BUE and diffusion are found under all the experimental conditions when using the original cutting inserts. These results are in line with our recently reported studies (X.-T. Duong et al., 2014; X. Duong et al., 2016; Seyed Ali Niknam, Saeid Kamalizadeh, et al., 2018).

Moreover, the flank wear with the sacrificial coating seems to increase faster under all the cutting speeds within less than 20 second. Right after the sacrificial coating disappears by chipping and friction, the wear evolutions are in the normal form. It is remarked that the thin film layer of Ni/B has still found to be rich on the flank wear face within the first wear period. Under the effect of hard particles on the contact interface the initial wear mechanism has significantly changed as discussed in the previous section. In this case, the adhesion wear and smoot layer, that have been reported to be resulted in the adhesion and diffusion mechanism, are found only in a certain moment of cutting, Figure 5-8 (a). The abrasion is however to be the dominant wear mechanism in almost all the investigated cutting conditions when using our plating coated layer. Therefore, within the first wear period, the flank wear on the sacrificial coating tools is greater than that of the original inserts under all the tested cutting conditions.

At the first moment of machining, the cutting edge deformed at low cutting speed of 20 m/min. The deformation tends to increase with the cutting forces and temperature. The increase in cutting forces and temperature leads to high contact stress and high friction between poorly conforming surfaces at the tool-workpiece interface. In this case, several hard particles broken from the workpiece material, subtract insert and sacrificial coating of Ni/B material are thus entrapped between the flank face and the material, resulting in abrasion wear. In the other hand, cracked materials in the damage zones are taken out with high wear rate due to overload of mechanical tensile stresses, as illustrated in Figure 5-12 and Figure 5-13. The abrasive wear is accelerated and depends on the percentage of the hard particle reinforcement in the workpiece material and the presence of Ni/B plating layer. The tool life during machining TiMMCs under the plating layer with of Ni/B material has not been completely recorded in this study. However, by depositing a

very thin material, around 100 nm of Ni/B as a sacrificial coating, on the cutting tool we have completely changed the initial wear mechanism from the adhesion to the abrasion wear mechanism. In order to control better the initial wear mechanism, various plating materials are recommended to change the chemical reaction within the initial wear period. This is indeed our future work to fulfill the new concept of plating on the cutting tool and recycle tooling as this method is fully feasible and very economic.

## 5.4 Conclusion

The cutting conditions have affected the tool wear behaviour of the new coating cutting tool. When the cutting speed and feed rate increase considerably, the abrasion wear is the dominant mechanism. At the lower cutting speed and feed rate, the main wear mechanism is adhesion. The reason of this phenomenon is explained in the previous part of this chapter. At low speed and low feed, high BUE formation and ploughing result in chipping at the tool edges. We also found that at high depth of cut, the hard particles of workpiece will abrade the tool due to the high cutting force.

Delamination was found at most of the cutting conditions, a poor adhesion of the coating to the base coating, low coverage at the edge and residual stresses can be given here for explanation.

The abrasion wear mechanism was mostly observed at the first initial wear period (0.5s) at lower and higher cutting speed. It is suggested that the presence of new coating material nickel-boron (Ni/B) affects to the chemical reaction and diffusion.

The adhesion wear mechanism has been reported as the most important mechanism of the initial wear period under the various cutting conditions while machining titanium metal matrix composites (X. Duong et al., 2016). However, at 0.5s of cutting time of experiments in this study, we did not really find the presence of the adhesion layer. The presence of our thin film sacrificial coating on the cutting tool has clearly changed the chemical wear behaviour and wear mechanism at the first wear period. We wish next to further discuss the effect of this coated layer on the tool life.

# CHAPTER 6 GENERAL DISCUSSTION AND CONCLUSION

This chapter summarizes the significant results obtained during the course of this study. As far as we know, this is the first time a sacrificial coating has successfully been coated on the carbide coated inserts. Such the coated layer contributes to change the initial wear mechanism during machining TiMMCs. The obtained results have suggested an interesting research direction on the tool wear and provided an alternative to recycle the used cutting tools through a simple and efficient coating method (i.e. electroless plating). We are therefore providing some recommendations that should be addressed for the future work.

## 6.1 Conclusion on electroless nickel plating onto PVD coated carbide tool

Electroless plating technique has been largely used in areas, from daily life to advanced technologies. However, its application is still limited in the field of cutting tool. This fact is understood by noting that electroless plating generally requires a surface pre-treatment using various aggressive chemical products. This work presents an easy diazonium-based chemical electroless nickel plating process onto the titanium nitride coated cutting tools without requiring any surface pre-treatment.

Because the surface coverage of the coated Ni-B film as well as the percentage of boron are essential for the wear resistance applications, we therefore have focused our attention on these parameters by using XPS, SEM and AFM techniques. Indeed, the plated surface is fully covered by a homogenous and continuous metallic film. Particularly for the wear resistance, the effect of boron content on hardness of electroless nickel-boron deposits is still an open subject in the literature. It was reported that hardness of nanocrystalline electroless nickel-boron coatings increases with increasing the boron content at least up to 8 weight % boron. In our case, the characterization of nickel-boron films reveals that they all contain the same amount of boron, 9.3 ± 0.1 % in weight. These 100-nm thick Ni-B films provide certain influence in the wear behaviors of the plated inserts. Remark that the chemical composition and thickness of nickel-boron film can be well controlled by changing the working condition of electroless plating process (bath composition, temperature, pH, plating time…). We believe that our simple and cost-effective

electroless plating strategy should be considered in the future studies to get more insight into the effect of the film composition and thickness with respect to the wear resistance.

## 6.2 Effect of cutting conditions on the tool wear during turning of TiMMCs

With the purpose of bringing out the role of the sacrificial coating layer we first concentrate on the effect of cutting conditions on the tool wear. The experimental design is performed in accordance with the response surface methodology (RSM) for the original coated inserts and sacrificial coating inserts. Based on the empirical equations the relationship between the cutting parameters and the flank wear are formed. In two cases, the cutting speed significantly affect the initial wear mechanism when turning TiMMCs. However, at the lower cutting speed, the initial wear under the sacrificial coating increases quicker than the original one. The initial wear VBB1 were evaluated within a range of 0.050 – 0.099 mm while VBB2 is 0.046 – 0.081. The improvement of the initial flank wear when using a sacrificial coating has been found under all the tested conditions. Additionally, at the center point of experiment where, the experiment was repeatedly tested (6 times), cutting speed of V = 45m/min, f = 0.15 mm/rev and ap 1.5mm, the initial wear reduced up to 26.8%. We also found that the improvement of the flank wear is negative at some points, even increases to 7.9%. Our ANOVA analysis for the behavior of wear evolution when using the sacrificial coating cutting tools confirms that the tool life can be predicted by adjusting the initial conditions. ***(objective 3).***

## 6.3 Conclusion on the effect of sacrifice Ni/B coated layer onto the tool wear during machining TiMMCs

The role of the Ni/B sacrificial coating versus the tool wear mechanism was discussed with assistance of the SEM AFM, EDS results. Under the same investigated cutting conditions preformed with the pristine inserts, the Ni/B electrolessly coated inserts presented better cutting performance than the PVD coated carbide, even up to 26%. The observed flank wear of new coating tool is observed less than tool wear of the original PVD coating tool. However, the adhesion or diffusion are no longer found at the first transition wear period due to the presence of the Ni/B which is still found to be rich, after 6.5 seconds. We have observed for the case of the sacrificial coating of Ni/B material that the abrasion is the most important mechanism under all experimental

conditions. As expected, the presence of our thin-film sacrificial coating on the cutting tool has clearly changed the chemical wear behavior and wear mechanism at the first wear period (**hypothesis 2, objective 2**). Since the wear shield has not been found at the first transition wear period when turning TiMMCs using our sacrifice plating layer, the improvement of tool life was thus not observed in this case. At some point of investigated, the wear rate when machining under the sacrifice of Ni/B layer tool is faster than that of the original carbide one. This phenomenon can be explained through the significant increases in cutting force and gradient temperature at the first moment of cutting at the tool-workpiece and machined surface interface. The cutting tool material tends to react chemically with titanium, then resulted in an adhesion of the workpiece material to the cutting inserts. However, after a very few moments of cutting, we observed on the flank face of the insert a portion nickel-boron of the sacrificial coating, which is approximatively estimated to ~100 nm on the flank face. Under this special working condition (high pressure and high temperature), all these elements which may presented here including Ni, B of the sacrificed layer, Ti, Al and TiC hard particles from workpiece material as well as Ti/AL-N from the PVD coated substrate are oxidized. The involvement of these elements in the machining process affected the thermal and chemical stability of the coating layer. The increase of cutting forces leads to high contact stress and high friction between the hard particles at the tool–machined surface interface which, in turn, resulted in abrasion under all the investigated cutting conditions, (**hypothesis 1, 2, objective 2**). Clearly, the presence of the Ni-B electrolessly plated layer onto PVD coated inserts may vary the wear mechanism. Therefore, it is recommended to pursuit the development of the new and efficient electroless plating methods to deposit various desired materials.

## 6.4 Research contributions

The new concept of plating a sacrificial layer which has been proved efficient through our primary results in this work may suggest an alternative to study the tool wear and tool life during a machining process. Another point to be underlined is that electroless plating can provide different desired materials, it is thus expected that we will be able to adjust the initial wear mechanism; hence predict and increase the tool life. Finally, it is worth reminding that our simple and cost-effective electroless plating strategy leaves is industrially feasible.

# REFERENCES


. 16 - Metal matrix, fibre–metal and ceramic matrix composites for aerospace applications. (2012). In A. P. Mouritz (Ed.), *Introduction to Aerospace Materials* (pp. 394-410): Woodhead Publishing.

Aramesh, M. (2015). *Machinability of titanium metal matrix composites (Ti-MMCs).* École Polytechnique de Montréal.

Astakhov, V. P. (2013). Tribology of Cutting Tools. In J. P. Davim (Ed.), *Tribology in Manufacturing Technology* (pp. 1-66). Berlin, Heidelberg: Springer Berlin Heidelberg.

Astakhov, V. P., & Davim, J. P. (2008). Tools (Geometry and Material) and Tool Wear *Machining: Fundamentals and Recent Advances* (pp. 29-57). London: Springer London.

Aziz, M., Redzuwan, B., Zaimi, M., Izamshah, R., Kasim, M., Md Ali, M. A., . . . Ishida, T. (2017). Mechanical properties and cutting performance of electroless ternary ni-w-p coated cutting tools. *Jurnal Teknologi, 79*. doi:10.11113/jt.v79.11291

Badoi, I., & Constantinescu, D. M. (2016). Wear Behavior of Metal Matrix Composites in Comparison to Sintered Metal Carbides. *Materials Today: Proceedings, 3*(4), 925-930. doi:https://doi.org/10.1016/j.matpr.2016.03.022

Bai, W., Roy, A., Sun, R., & Silberschmidt, V. V. (2019). Enhanced machinability of SiC-reinforced metal-matrix composite with hybrid turning. *Journal of Materials Processing Technology, 268*, 149-161. doi:https://doi.org/10.1016/j.jmatprotec.2019.01.017

Bejjani, R. (2012). *Machinability and modeling of cutting mechanism for titanium metal matrix composites.* École Polytechnique de Montréal.

Bejjani, R., Balazinski, M., Attia, H., Plamondon, P., & L'Espérance, G. (2016). Chip formation and microstructure evolution in the adiabatic shear band when machining titanium metal matrix composites. *International Journal of Machine Tools and Manufacture, 109*, 137-146.

Bhushan, R. K., Kumar, S., & Das, S. (2010). Effect of machining parameters on surface roughness and tool wear for 7075 Al alloy SiC composite. *The International Journal of Advanced Manufacturing Technology, 50*(5-8), 459-469.

Byrne, G., Dornfeld, D., & Denkena, B. (2003). Advancing cutting technology. *CIRP Annals, 52*(2), 483-507.

Calamba, K. M., Johansson Jõesaar, M. P., Bruyère, S., Pierson, J. F., Boyd, R., Andersson, J. M., & Odén, M. (2019). The effect of nitrogen vacancies on initial wear in arc deposited (Ti0.52,Al0.48)Ny, (y < 1) coatings during machining. *Surface and Coatings Technology, 358*, 452-460. doi:https://doi.org/10.1016/j.surfcoat.2018.11.062

Campbell, F. C. (2006). Metal Matrix Composites *Manufacturing Technology for Aerospace Structural Materials* (pp. 419-457). Oxford: Elsevier Science.

Cao, H.-c., & Liang, Y.-l. (2020). The microstructures and mechanical properties of graphene-reinforced titanium matrix composites. *Journal of Alloys and Compounds, 812*, 152057. doi:https://doi.org/10.1016/j.jallcom.2019.152057

Choudhury, I. A., & El-Baradie, M. A. (1999). Machinability assessment of inconel 718 by factorial design of experiment coupled with response surface methodology. *Journal of Materials Processing Technology, 95*(1–3), 30-39. doi:10.1016/s0924-0136(99)00085-0

Davim, J. P. (2008). *Machining: fundamentals and recent advances*: Springer Science & Business Media.

Deng, Y., Chen, W., Li, B., Wang, C., Kuang, T., & Li, Y. (2020). Physical vapor deposition technology for coated cutting tools: A review. *Ceramics International, 46*(11, Part B), 18373-18390. doi:https://doi.org/10.1016/j.ceramint.2020.04.168

Dobrzański, L., & Dołżańska, B. (2010). Hardness to toughness relationship on WC-Co tool gradient materials evaluated by Palmqvist method. *Archives of Materials Science and Engineering, Vol. 43, nr 2*, 87-93.

Duong, X.-T., Balazinski, M., & Mayer, R. (2014). *Chaotic tool wear during machining of titanium metal matrix composite (TiMMCs).* Paper presented at the ASME 2014 International Mechanical Engineering Congress and Exposition.

Duong, X., Mayer, J., & Balazinski, M. (2016). Initial tool wear behavior during machining of titanium metal matrix composite (TiMMCs). *International Journal of Refractory Metals and Hard Materials, 60*, 169-176.

Duong, X. T. (2015a). *Chaos Theory applied to analyze tool wear during machining of titanium metal matrix composite (TiMMCs).* École Polytechnique de Montréal.

Duong, X. T. (2015b). *Chaos theory applied to analyze tool wear during machining of titanium metal matrix composite (TiMMCs).* (PhD), Polytechnique Montreal - University of Montreal

Duong, X. T., & Duc, T. (2013). EFFECT OF CUTTING CONDITION ON TOOL WEAR AND SURFACE ROUGHNESS DURING MACHINING OF INCONEL 718. *International Journal of Advanced Engineering Technology E-ISSN 0976-3945, 108*, 112.

Escaich, C., Shi, Z., Baron, L., & Balazinski, M. (2020). Machining of Titanium Metal Matrix Composites: Progress Overview. *Materials, 13*(21).

Fan, J., & Njuguna, J. (2016). 1 - An introduction to lightweight composite materials and their use in transport structures. In J. Njuguna (Ed.), *Lightweight Composite Structures in Transport* (pp. 3-34): Woodhead Publishing.

Fuentes, G. G. (2010). Surface Engineering and Micro-manufacturing. *Micromanufacturing Engineering and Technology*, 459-486.

Haghshenas, M. (2016). Metal–Matrix Composites *Reference Module in Materials Science and Materials Engineering*: Elsevier.

Hayat, M. D., Singh, H., He, Z., & Cao, P. (2019). *Titanium metal matrix composites: An overview.*

Heath, P. J. (2001). Developments in applications of PCD tooling. *Journal of Materials Processing Technology, 116*(1), 31-38. doi:https://doi.org/10.1016/S0924-0136(01)00837-8

Hosseini, A., & Kishawy, H. (2019). *Chapter 2 Cutting Tool Materials and Tool Wear*.

Kamali Zadeh, S. (2016). *Initial tool wear mechanisms in turning of titanium metal matrix composites.* École Polytechnique de Montréal.

Ma, J., Luo, D., Liao, X., Zhang, Z., Huang, Y., & Lu, J. (2020). Tool wear mechanism and prediction in milling TC18 titanium alloy using deep learning. *Measurement*, 108554. doi:https://doi.org/10.1016/j.measurement.2020.108554

Mallick, P. K. (2012). 2 - Advanced materials for automotive applications: an overview. In J. Rowe (Ed.), *Advanced Materials in Automotive Engineering* (pp. 5-27): Woodhead Publishing.

Memarianpour, M., Niknam, S. A., Turenne, S., & Balazinski, M. (2018). *Initial Tool Wear Mechanism in Dry and Lubricated Turning of Inconel 718.* Paper presented at the International Conference on Engineering Research and Applications.

Montazeri, S., Aramesh, M., & Veldhuis, S. C. (2020). Novel application of ultra-soft and lubricious materials for cutting tool protection and enhancement of machining induced

surface integrity of Inconel 718. *Journal of Manufacturing Processes, 57*, 431-443. doi:https://doi.org/10.1016/j.jmapro.2020.07.002

Mu, X. N., Zhang, H. M., Cai, H. N., Fan, Q. B., Wu, Y., Fu, Z. J., & Wang, Q. X. (2017). Hot Pressing Titanium Metal Matrix Composites Reinforced with Graphene Nanoplatelets through an In-Situ Reactive Method. *2nd International Conference on Composite Materials and Material Engineering (Iccmme2017), 1846*. doi:Unsp 020013-1

10.1063/1.4983594

Munir, K. S., Kingshott, P., & Wen, C. (2015). Carbon Nanotube Reinforced Titanium Metal Matrix Composites Prepared by Powder Metallurgy-A Review. *Critical Reviews in Solid State and Materials Sciences, 40*(1), 38-55. doi:10.1080/10408436.2014.929521

Nicholls, C. J., Boswell, B., Davies, I. J., & Islam, M. N. (2017). Review of machining metal matrix composites *The International Journal of Advanced Manufacturing Technology* (Vol. 90, pp. 2429-2441).

Niknam, S. A., Kamalizadeh, S., Asgari, A., & Balazinski, M. (2018). Turning titanium metal matrix composites (Ti-MMCs) with carbide and CBN inserts. *The International Journal of Advanced Manufacturing Technology, 97*(1), 253-265. doi:10.1007/s00170-018-1926-9

Niknam, S. A., Kamalizadeh, S., Asgari, A., & Balazinski, M. (2018). Turning titanium metal matrix composites (Ti-MMCs) with carbide and CBN inserts. *International Journal of Advanced Manufacturing Technology, 97*(1-4), 253-265. doi:10.1007/s00170-018-1926-9

Niknam, S. A., Khettabi, R., & Songmene, V. (2014). Machinability and machining of titanium alloys: a review *Machining of titanium alloys* (pp. 1-30): Springer.

Niknam, S. A., Kouam, J., Songmene, V., & Balazinski, M. (2018). Dry and Semi-Dry Turning of Titanium Metal Matrix Composites (Ti-MMCs). *Procedia CIRP, 77*, 62-65. doi:https://doi.org/10.1016/j.procir.2018.08.215

Pramanik, A., & Littlefair, G. (2015). Machining of Titanium Alloy (Ti-6Al-4V)—Theory to Application. *Machining Science and Technology, 19*(1), 1-49. doi:10.1080/10910344.2014.991031

Saba, F., Zhang, F., Liu, S., & Liu, T. F. (2019). Reinforcement size dependence of mechanical properties and strengthening mechanisms in diamond reinforced titanium metal matrix composites. *Composites Part B-Engineering, 167*, 7-19. doi:10.1016/j.compositesb.2018.12.014

Salur, E., Aslan, A., Kuntoglu, M., Gunes, A., & Sahin, O. S. (2019). Experimental study and analysis of machinability characteristics of metal matrix composites during drilling. *Composites Part B: Engineering, 166*, 401-413. doi:https://doi.org/10.1016/j.compositesb.2019.02.023

Stephenson, D. A., & Agapiou, J. S. (2016). *Metal cutting theory and practice*: CRC press.

Vereschaka, A., Gurin, V., Oganyan, M., Oganyan, G., Bublikov, J., & Shein, A. (2019). Increase in tool life for end milling titanium alloys using tools with multilayer composite nanostructured modified coatings. *Procedia CIRP, 81*, 1412-1416. doi:https://doi.org/10.1016/j.procir.2019.04.173

Vitry, V., & Delaunois, F. (2015). 7 - Nanostructured electroless nickel-boron coatings for wear resistance. In M. Aliofkhazraei (Ed.), *Anti-Abrasive Nanocoatings* (pp. 157-199): Woodhead Publishing.

Vu, N. P., Duong, X. T., Ly, V. A., Nguyen, D. C., Tran, M. D., Phan, Q. T., . . . Le, X. T. (2018). Electroless nickel plating onto Plexiglas® through simple covalent grafting of vinylpyridine seed layer. *Materials & Design, 144*, 151-158.

Woon, K. S. (2021). High Performance Machining of Metal Matrix Composites *Reference Module in Materials Science and Materials Engineering*: Elsevier.

Xuan-Truong, D., & Minh-Duc, T. (2013). Effect of cutting condition on tool wear and surface roughness during machining of Inconel 718. *International Journal of Advanced Engineering Technology/IV/III/July-Sept, 108*, 112.

Zeb, G., Duong, T. L., Balazinski, M., & Le, X. T. (2020). *Direct Electroless Deposition of Nickel onto Silicon Nitride Ceramic: A Novel Approach for Copper Metallization of Micro-/Nano-fabricated Devices.*

Zeb, G., Duong, X. T., Vu, N. P., Phan, Q. T., Nguyen, D. T., Ly, V. A., . . . Le, X. T. (2017). Chemical metallization of KMPR photoresist polymer in aqueous solutions. *Applied Surface Science, 407*, 518-525.

Zeb, G., Zafar, M., Palacin, S., & Le, X. T. (2017). An Application of Diazonium-Induced Anchoring Process in the Fabrication of Micro-Electromechanical Systems. *Advanced Materials Technologies, 2*(12), 1700159. doi:https://doi.org/10.1002/admt.201700159

Zhao, J., & Liu, Z. (2020). Influences of coating thickness on cutting temperature for dry hard turning Inconel 718 with PVD TiAlN coated carbide tools in initial tool wear stage. *Journal of Manufacturing Processes, 56*, 1155-1165. doi:https://doi.org/10.1016/j.jmapro.2020.06.010

# APPENDIX A

## REFEREED JOURNAL PAPERS

- Zeb, G., Duong, T. L., Balazinski, M., & Le, X. T. (2020). *Direct Electroless Deposition of Nickel onto Silicon Nitride Ceramic: A Novel Approach for Copper Metallization of Micro-/Nano-fabricated Devices*